

Spring 2004

Ultimate Strength Prediction in Fiberglass/Epoxy Beams Subjected to Three-Point Bending Using Acoustic Emission and Neural Networks

Michele D. Dorfinan
Embry-Riddle Aeronautical University - Daytona Beach

Follow this and additional works at: <https://commons.erau.edu/db-theses>



Part of the [Aerospace Engineering Commons](#)

Scholarly Commons Citation

Dorfinan, Michele D., "Ultimate Strength Prediction in Fiberglass/Epoxy Beams Subjected to Three-Point Bending Using Acoustic Emission and Neural Networks" (2004). *Theses - Daytona Beach*. 294.
<https://commons.erau.edu/db-theses/294>

This thesis is brought to you for free and open access by Embry-Riddle Aeronautical University – Daytona Beach at ERAU Scholarly Commons. It has been accepted for inclusion in the Theses - Daytona Beach collection by an authorized administrator of ERAU Scholarly Commons. For more information, please contact commons@erau.edu.

**ULTIMATE STRENGTH PREDICTION IN FIBERGLASS/EPOXY BEAMS
SUBJECTED TO THREE-POINT BENDING USING ACOUSTIC EMISSION
AND NEURAL NETWORKS**

by

Michele D. Dorfman

A Thesis Submitted to the Graduate Studies Office
in Partial Fulfillment of the Requirements for the Degree
of Master of Science in Aerospace Engineering

Embry-Riddle Aeronautical University
Daytona Beach, Florida
Spring 2004

UMI Number: EP32062

INFORMATION TO USERS

The quality of this reproduction is dependent upon the quality of the copy submitted. Broken or indistinct print, colored or poor quality illustrations and photographs, print bleed-through, substandard margins, and improper alignment can adversely affect reproduction.

In the unlikely event that the author did not send a complete manuscript and there are missing pages, these will be noted. Also, if unauthorized copyright material had to be removed, a note will indicate the deletion.

UMI[®]

UMI Microform EP32062
Copyright 2011 by ProQuest LLC
All rights reserved. This microform edition is protected against
unauthorized copying under Title 17, United States Code.

ProQuest LLC
789 East Eisenhower Parkway
P.O. Box 1346
Ann Arbor, MI 48106-1346


**ULTIMATE STRENGTH PREDICTION IN FIBERGLASS/EPOXY BEAMS
SUBJECTED TO THREE-POINT BENDING USING ACOUSTIC EMISSION
AND NEURAL NETWORKS**

by

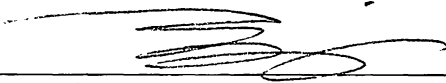
Michele D. Dorfman

This thesis was prepared under the direction of the candidate's thesis committee chairmen, Dr. Eric v. K. Hill and Dr. Yi Zhao, Department of Aerospace Engineering, and has been approved by the members of her thesis committee. It was submitted to the School of Graduate Studies and Research and was accepted in partial fulfillment of the requirements for the degree of Master of Science in Aerospace engineering.

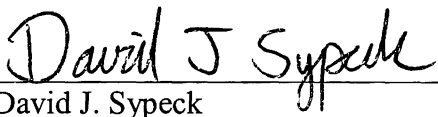
THESIS COMMITTEE:



Dr. Eric v. K. Hill
Chairman




Dr. Yi Zhao
Chairman



Dr. David J. Sypeck
Member



Graduate Program Coordinator, MSAE 6/2/04
Date



Department Chair, Aerospace Engineering 6/8/04
Date

ACKNOWLEDGEMENTS

I would first like to thank my thesis committee, Dr. Eric v. K. Hill, Dr. Yi Zhao and Dr. David J. Sypeck for their time, advice and encouragement throughout my thesis research. Without them, none of this would have been possible. I would also like to thank Dr. Hill and Dr. Zhao for providing me with the teaching assistantships that financed my graduate education. A special thanks must go to the following students for their help throughout my thesis research: Alexis Farfaro for all his help in the preliminary stages of this project; Roiann Nimis for all her time spent from start to finish of this project, but especially the many hours she spent with me optimizing the backpropagation neural network; Tuan-Khoi Nguyen for his help with everything, most importantly his help manufacturing the beams; and finally, Darryl Hearn for all his help, but especially the many hours he spent perfecting the Kohonen self organizing map. Last, but definitely not least, I would like to thank my parents, Howard and Carol Dorfman, for all of their support and encouragement throughout my graduate studies.

ABSTRACT

Author: Michele D. Dorfman
Title: Ultimate Strength Prediction in Fiberglass/Epoxy Beams Subjected to Three-Point Bending Using Acoustic Emission and Neural Networks
Institution: Embry-Riddle Aeronautical University
Degree: Master of Science in Aerospace Engineering
Year: 2004

The research presented herein demonstrates the feasibility of predicting ultimate strengths in composite beams subjected to 3-point bending using a neural network analysis of acoustic emission (AE) amplitude distribution data. Fifteen unidirectional fiberglass/epoxy beams were loaded to failure in a 3-point bend test fixture in an MTS load frame. Acoustic emission data were recorded from the onset of loading until failure. After acquisition, the acoustic emission data were filtered to include only data acquired up to 80 percent of the average ultimate load.

A backpropagation neural network was constructed to predict the ultimate failure load using these AE amplitude distribution data. Architecturally, the network consisted of a 61 processing element input layer for each of the event frequencies, a 13 processing element hidden layer for mapping, and a single processing element output layer for predicting the ultimate load. The network, trained on seven beams, was able to predict ultimate loads in the remaining eight beams with a worst case error of +4.34 percent, which was within the desired goal of ± 5 percent.

A second analysis was performed using a Kohonen self organizing map and multivariate statistical analysis. A Kohonen self organizing map was utilized to classify the AE data into 4 failure mechanisms. Then multivariate statistical analysis was performed using the number of hits associated with each failure mechanism to develop a prediction equation. The prediction equation was able to predict the ultimate failure load with a worst case error of -11.34 percent, which was well outside the desired goal of ± 5 percent. This was thought to be the result of noisy or sparse data, since statistical predictions are inherently sensitive to both, whereas backpropagation neural networks are not.

TABLE OF CONTENTS

	Page
Signature Page	ii
Acknowledgements.....	iii
Abstract.....	iv
Table of Contents.....	v
List of Tables	vii
List of Figures.....	viii
CHAPTER 1 INTRODUCTION.....	1
1.1 Overview.....	1
1.2 Previous Research.....	2
1.3 Current Approach.....	3
CHAPTER 2 BACKGROUND THEORY.....	5
2.1 Material System	5
2.3 Acoustic Emission	6
2.3.1 Event Parameters	8
2.3.2 Failure Mechanisms.....	10
2.3.3 Amplitude Distribution.....	11
2.4 Neural Networks.....	13
2.4.1 Backpropagation Neural Networks.....	15
2.4.2 Kohonen Self Organizing Maps.....	19
CHAPTER 3 EXPERIMENTAL PROCEDURE.....	23
3.1 Fiberglass/Epoxy Beams.....	23
3.2 Test Setup.....	25

3.2.1 Specimen Setup.....	27
3.2.2 MTS Load Frame Setup.....	27
3.3 Data Acquisition	28
3.4 Test Procedure	29
CHAPTER 4 ANALYSIS AND RESULTS.....	32
4.1 Acoustic Emission Data.....	32
4.2 Backpropagation Neural Network	36
4.3 Kohonen Self Organizing Map.....	43
4.4 Multivariate Statistical Analysis.....	52
CHAPTER 5 CONCLUSIONS AND RECOMMENDATIONS.....	55
5.1 Conclusions.....	55
5.2 Recommendations.....	56
REFERENCES	57
BIBLIOGRAPHY	58
APPENDIX.....	59
A Acoustic Emission Data Plots.....	59
B Neural Network Parameter Definitions.....	75
C Backpropagation Neural Network Results.....	83

LIST OF TABLES

	Page
Table 2.1	AE parameters and associated failure mechanisms in fiberglass/epoxy11
Table 4.1	Ultimate loads and corresponding AE hits.....32
Table 4.2	AE hits associated with percentage of average ultimate load33
Table 4.3	Training set.....36
Table 4.4	Testing set37
Table 4.5	Network parameters38
Table 4.6	Final network parameters42
Table 4.7	Backpropagation neural network results43
Table 4.8	20 x 20 SOM network parameters.....44
Table 4.9	20 x 20 SOM results for energy, duration, and amplitude45
Table 4.10	5 x 1 SOM network parameters.....46
Table 4.11	5 x 1 SOM results for energy, duration, and amplitude47
Table 4.12	4 x 1 SOM network parameters.....48
Table 4.13	4 x 1 SOM results for energy, duration, and amplitude48
Table 4.14	4 x 1 SOM results for 80% data51
Table 4.15	Multiple linear regression inputs.....53
Table 4.16	Multiple linear regression analysis results54

LIST OF FIGURES

	Page
Figure 2.1 Complete acoustic emission system	7
Figure 2.2 Acoustic emission transducer	7
Figure 2.3 Acoustic emission waveform and parameters	9
Figure 2.4 Amplitude distribution histogram	12
Figure 2.5 Processing element (neuron)	13
Figure 2.6 Transfer functions	14
Figure 2.7 Generic neural network architecture	14
Figure 2.8 Backpropagation neural network	15
Figure 2.9 Kohonen self organizing map	19
Figure 3.1 Beams curing at room temperature	24
Figure 3.2 Complete test setup	26
Figure 3.3 MTS setup without beam specimen	26
Figure 3.4 Transducers mounted on specimen	27
Figure 3.5 Waveform with setup parameters.....	29
Figure 3.6 Test specimen prior to loading	30
Figure 3.7 Test specimen after failure	30
Figure 3.8 Load vs. displacement plot.....	31
Figure 4.1 Amplitude distribution plot	34
Figure 4.2 Duration vs. amplitude plot.....	35
Figure 4.3 Duration vs. counts plot	35
Figure 4.4 Optimizing number of processing elements in hidden layer plot.....	38

Figure 4.5	Optimizing F' offset plot.....	39
Figure 4.6	Optimizing transition point plot	39
Figure 4.7	Optimizing the momentum plot	40
Figure 4.8	Optimizing hidden layer learning coefficient plot	40
Figure 4.9	Optimizing output layer learning coefficient plot	41
Figure 4.10	Optimizing learning coefficient ratio plot.....	41
Figure 4.11	Optimizing RMS error plot	42
Figure 4.12	X-Y coordinate plot.....	45
Figure 4.13	Sorted duration vs. amplitude plot	49
Figure 4.14	Sorted amplitude distribution plot.....	50
Figure 4.15	Sorted duration vs. amplitude plot for 80% data.....	52

CHAPTER 1

INTRODUCTION

1.1 OVERVIEW

In today's aircraft industry, the materials available to designers have always had a strong impact on how aircraft are designed and built. The basic fundamentals of flight, such as the ratios of lift to drag, and thrust to weight have, unsurprisingly, dictated the choice of materials used. The materials chosen have been generally based on their strength to weight criteria.

Composite materials have made the primary impact in the aircraft industry market today. The greatest advantage of these materials is their high strength-to-weight ratios. Composites can produce weight savings of up to 25% over their metallic counterparts [1]. Due to the increased use of composite materials, research in quality control of these structures must be a continuing process.

Proof loading is the application of a load, frequently in excess of the maximum service load, to a component or structure in order to assure safety [2]. The theory behind proof loading is the assumption that if the structure does not fail during the proof test, it will not fail in service.

The research herein involves proof loading composite beams in 3-point bending to 80 percent of their average ultimate strength. Acoustic emission nondestructive testing combined with a neural network analysis were then used to predict the ultimate strengths in fiberglass/epoxy beams.

1.2 PREVIOUS RESEARCH

Previous research has shown that AE data combined with the use of neural networks can be used to create a prediction model for ultimate loads in various applications. Hill, Walker and Rowell [3] tested a set of eighteen ASTM standard 145 mm (5.75 in.) diameter filament wound graphite/epoxy pressure vessels. Acoustic emission amplitude distribution data taken during hydroproof up to 25 percent of the expected burst pressure were used as inputs for a backpropagation neural network. The network, trained on nine bottles, was able to predict burst pressures in the remaining eight bottles with a worst case error of -3.89 percent.

Fisher and Hill [4] tested a set of eleven ASTM standard 145 mm (5.75 in.) diameter filament wound fiberglass/epoxy pressure vessels. Two of these bottles contained simulated manufacturing defects which lowered their burst pressures significantly. Again, acoustic emission amplitude distribution data taken during hydroproof up to 25 percent of the expected burst pressure were used as inputs for a backpropagation neural network. The network, trained on seven bottles (one containing a defect), was able to predict burst pressures in the remaining four bottles (one containing a defect) with a worst case error of +14.7 percent. When the defective bottles were removed from

consideration, the worst case prediction error dropped to -2.1 percent. It was concluded that more defective bottles would need to be tested in order to increase the prediction accuracy.

Fatzinger and Hill [5] tested a set of ten fiberglass/epoxy I-beams loaded in cantilever fashion with a hydraulic ram. Two of these beams were manufactured using a different resin type. Acoustic emission amplitude distribution data taken during loading up to 50 percent of the theoretical ultimate load were used as inputs for a backpropagation neural network. The network, trained on five beams (one from the different resin type), was able to predict ultimate loads in the remaining beams with a worst case error of -10.6 percent. A Kohonen self organizing map was utilized to classify the AE data into failure mechanisms. Then a multivariate statistical analysis was performed using the percentage of AE hits associated with each failure mechanism along with the epoxy type to develop a prediction equation for ultimate load. The multivariate statistical analysis resulted in a prediction equation that had a worst case error of +36.0 percent. The large error for the statistical analysis was probably due to sparse data.

1.3 CURRENT APPROACH

The current approach is similar to those previously mentioned; however, the beams were loaded in 3-point bending. Fifteen unidirectional fiberglass/epoxy beams were loaded to failure in an MTS load frame using a 3-point bend test fixture. Acoustic emission amplitude distribution data taken during loading up to 80 percent of the average ultimate load were used as inputs for a backpropagation neural network. The network was trained

on seven beams, and tested on the remaining eight. Then a second analysis was performed using a Kohonen self organizing map and multivariate statistical analysis. The Kohonen self organizing map was utilized to classify the AE data into failure mechanisms. Then multivariate statistical analysis was performed using the number of hits associated with each failure mechanism to develop a prediction equation.

CHAPTER 2

BACKGROUND THEORY

2.1 MATERIAL SYSTEM

The material system used in this research was Saint-Gobain Vetrotex America, Inc. RO99-625 unidirectional glass roving and West System 105 epoxy resin with a West System 206 slow hardener.

According to the manufacturer, RO99-625 is a high-performance, multi-resin-compatible reinforcement used for filament winding fuel and chemical storage tanks, large diameter pipe, water treatment vessels, pressure vessels, reverse osmosis tubes and electrical fuse tubes. It has been specifically designed to achieve optimum results in polyester, vinylester, phenolic and epoxy resin systems.

According to West System, 105 epoxy resin is a clear, pale yellow, low-viscosity liquid epoxy resin. When cured, the resin is clear. It can be cured in a wide variety of temperature ranges to form a high-strength solid with excellent moisture resistance. It is designed to wet out and bond with wood fiber, fiberglass, reinforcing fabrics and a variety of metals. The 206 slow hardener is a low-viscosity epoxy curing agent for use when extended working and cure time is needed or to provide adequate working time at higher temperatures. When combined with 105 resin in a five-part resin to one-part

hardener ratio, the cured resin/hardener mixture yields a rigid, high-strength, moisture-resistant solid with excellent bonding and coating properties.

2.3 ACOUSTIC EMISSION

Acoustic emission (AE) can be defined as the transient elastic waves generated by the rapid release of energy from sources within a stressed material. The most common sources of this energy release in a composite structure are matrix cracking, delaminations and fiber breaks [6]. External sources such as mechanical noises can also be detected. In most cases, the structure is undergoing tension, compression, bending, or pressurization to generate the stresses needed to cause acoustic emissions. The transient elastic stress waves travel outward from the growth source. Acoustic emission transducers are used to convert the mechanical stress waves into usable electrical voltage signals. An AE data acquisition system can be utilized to convert the electrical voltage signals to AE quantification parameters. These AE parameters can be represented graphically and used in analyses. A typical AE system is shown in Figure 2.1, and a detailed view of the AE transducer is given in Figure 2.2.

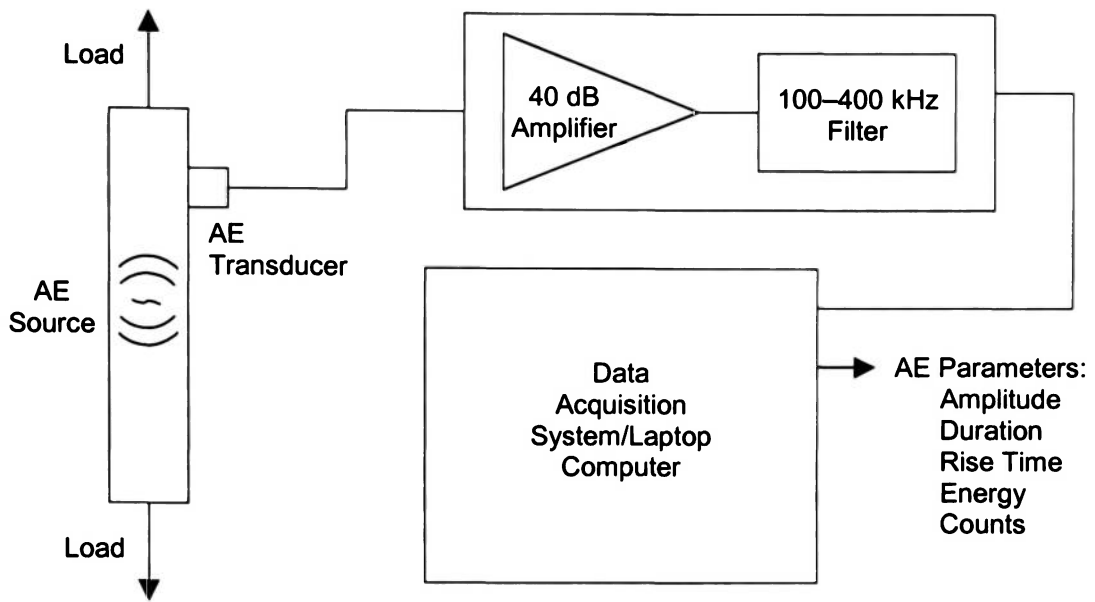


Figure 2.1 Complete acoustic emission system

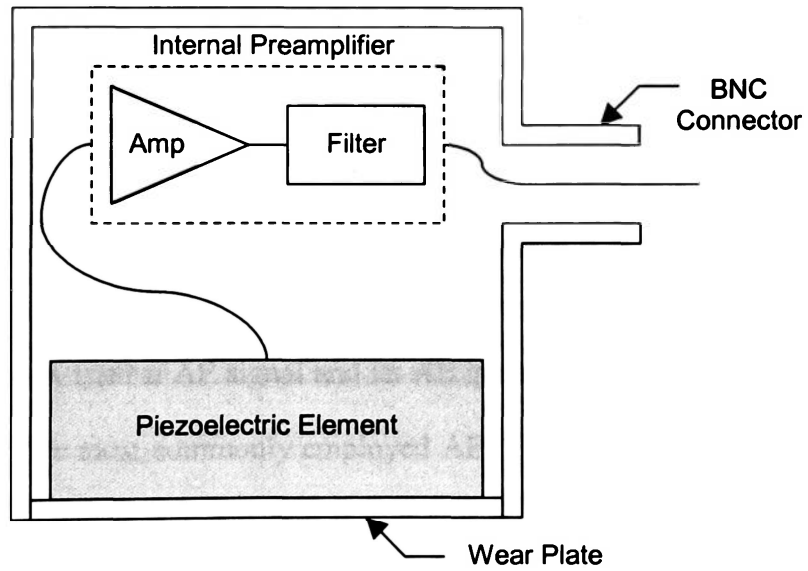


Figure 2.2 Acoustic emission transducer

An AE system works in the following way. A mechanical stress wave is generated by the rapid release of energy due to the flaw growth caused by an applied stress. Most AE transducers, which use a piezoelectric element for transduction, convert the mechanical stress wave into an electrical voltage signal. The electrical voltage signal is then passed through a preamplifier and a frequency filter. The preamplifier typically provides a gain of 100 (40 dB) and includes a high-pass or bandpass filter. The most common bandpass is 100-300 kHz, encompassing the 150 kHz resonant frequency of the most commonly used sensor [7]. It filters out the signals below 100 kHz and above 300 kHz. This eliminates low frequency background noise and high frequency noise caused by electromagnetic interference, but also limits the range of AE signals that can be detected. The amplified and filtered voltage signal is then fed into the data acquisition system, where it is amplified again and stored for future analysis. The data acquisition system extracts information about the voltage signal and generates AE quantification parameters. These AE parameters are displayed on the computer screen in the form of correlation plots or numerical tables.

2.3.1 Event Parameters

A typical AE signal or hit can be represented as a complex, damped, sinusoidal voltage versus time trace. A typical AE signal and its AE quantifying parameters can be seen in Figure 2.3. The five most commonly employed AE parameters are amplitude, duration, counts, rise time, and energy.

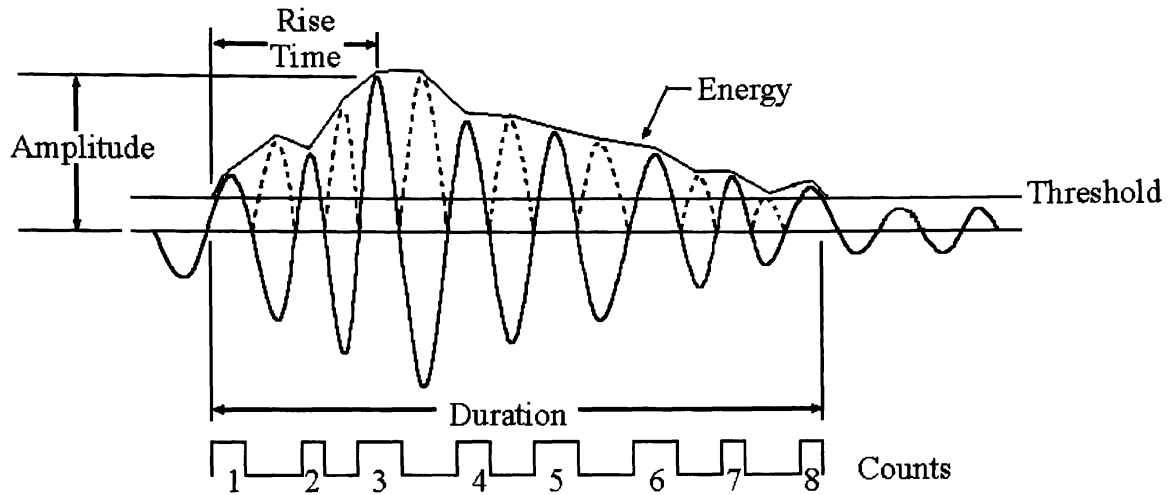


Figure 2.3 Acoustic emission waveform and parameters

These parameters are defined as follows. The amplitude is the largest voltage peak in the signal waveform. Amplitude is measured in decibels [dB]. The duration is the length of the hit, from the first crossing of the threshold to the last crossing of the threshold. Duration is measured in microseconds [μs]. Counts is defined as the number of times the signal crosses the threshold. Counts is also known as ringdown counts or threshold crossing counts. Rise time is the time from the start of the hit to its peak amplitude. Rise time is measured in microseconds [μs]. Energy, also known as MARSE, is the measured area under the rectified waveform. Energy is measured in energy counts.

Threshold is another essential parameter in acoustic emissions signal analysis. The threshold is an adjustable amplitude setting that determines when the data acquisition system starts recording hits. The sensitivity of the system is determined by the threshold setting. Unwanted background noises can be eliminated by setting the threshold above the amplitude of the unwanted noise, but also below the amplitude of the AE data needed.

2.3.2 Failure Mechanisms

The three primary failure mechanisms in composite materials are matrix cracking, delaminations, and fiber breaks. These failure mechanisms have been characterized by Hill [8] using the magnitude of the amplitude, duration, counts, rise time, and energy associated with each AE hit in fiberglass/epoxy pressure vessels.

The first primary failure mechanism is matrix cracking. There are two types of matrix cracking, transverse and longitudinal. Transverse matrix cracking is perpendicular to the fiber orientation, and longitudinal matrix cracking is parallel to the fiber orientation. Transverse matrix cracking hits in fiberglass/epoxy pressure vessels exhibit low amplitude, energy, and counts with short durations [8]. Longitudinal matrix cracking (fiber/matrix debonding) hits exhibit medium amplitude and energy with high counts and long durations. Matrix cracking occurs throughout the loading of the test specimen and is usually the least damaging of the three failure mechanisms.

The second primary failure mechanism is delaminations. Delaminations occur mostly in specimens subjected to bending. When delaminations occur in fiberglass bottles, they release very high amplitude, high energy signals with long durations and a high number of counts [8].

The third primary failure mechanism is fiber breaks. Fiber break signals in fiberglass pressure vessels exhibit high amplitudes and high energies with short to medium durations and low to medium counts [8]. Fiber breaks usually occur at the end of the

loading cycle and are the most damaging of the three failure mechanisms. The following table illustrates the relative magnitudes of the AE parameters associated with each of the three primary failure mechanisms in fiberglass/epoxy pressure vessels.

Table 2.1 AE parameters and associated failure mechanisms in fiberglass/epoxy pressure vessels [8]

AE Parameter	Transverse Matrix Cracking	Longitudinal Matrix Cracking	Delaminations	Fiber Breaks
Amplitude	Low	Medium	High	Low-Medium
Energy	Low	Medium	High	Very High
Counts	Low	High	High	Medium-High
Duration	Short	Long	Long	Short- Medium

2.3.3 Amplitude Distribution

As stated previously, the amplitude is the largest voltage peak in the signal waveform. Acoustic emission signal sources can range from 1 microvolt to 10 volts; therefore, it is convenient to represent the amplitude on a logarithmic scale. Amplitude is customarily expressed in decibels relative to 1 microvolt at the transducing element. Amplifier gain is then given by

$$\Delta dB = 20 \log \frac{V_{out}}{V_{in}} \text{ [dB]},$$

where V_{out} = output voltage [dB] and V_{in} = input voltage [dB]. The detectable range of AE amplitudes is on the scale of 0-100 decibels, and typical threshold settings for composite materials are 45-60 decibels.

Acoustic emission amplitude data can be graphed into a hits vs. amplitude histogram. Figure 2.4 shows a typical [differential] amplitude distribution plot for the fiberglass/epoxy beams used in this research. Previous research by Kouvarakos and Hill [6] has shown that the AE failure mechanisms are represented by the humps that make up the amplitude distribution. These humps have a tendency to overlap each other making it difficult to differentiate between the failure mechanisms on the amplitude histogram.

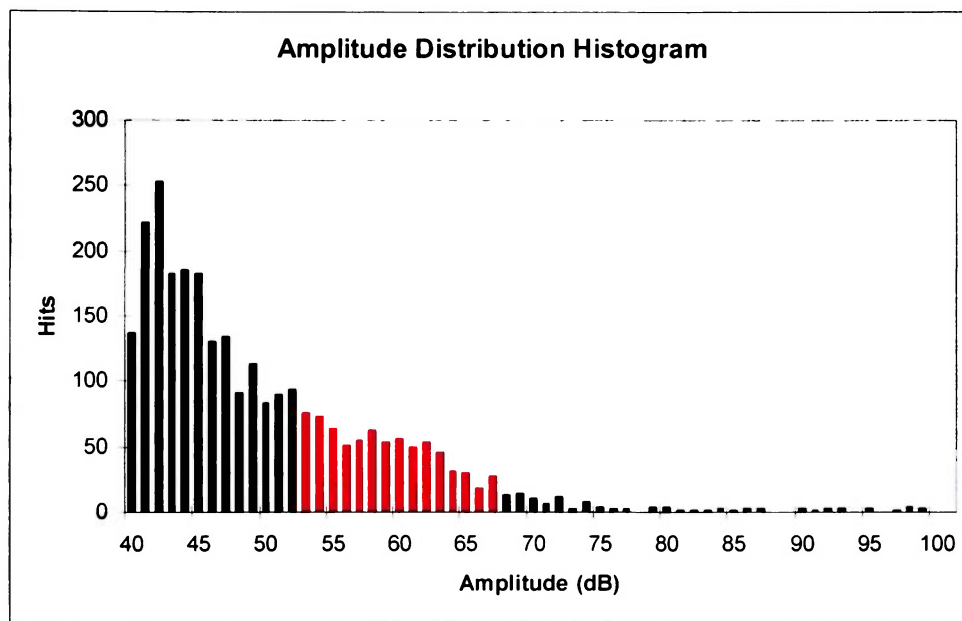


Figure 2.4 Amplitude distribution histogram

Neural networks can be useful in analyzing acoustic emission data. The amplitude distribution data can be input into a backpropagation neural network for prediction. The neural network can associate the hit frequencies with an ultimate load. Moreover, Kohonen self organizing maps can be used to classify the failure mechanisms into amplitude ranges.

2.4 NEURAL NETWORKS

An artificial neural network is a mathematical modeling and information processing tool with performance characteristics similar to those of a biological neural network. An artificial neural network, like a biological neural network, consists of a network of massively parallel, interconnected processing elements (PE) or neurons. A typical PE is shown in Figure 2.5.

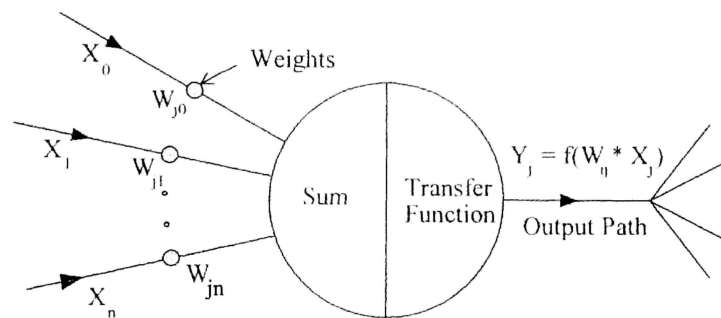


Figure 2.5 Processing element (neuron)

Each PE receives a number of input signals that may or may not generate an output signal based upon the given inputs. Each input has a relative weight associated with it such that the effective input to the PE is a summation of the inputs multiplied by their associated weights. This value is then modified by a transfer or activation function (Figure 2.6) and passed directly to the output path of the processing element. These outputs can either be excitatory or inhibitory. An excitatory output will cause the PE to fire; an inhibitory output will keep the PE from firing. This output signal can then be interconnected to the input paths of other processing elements.

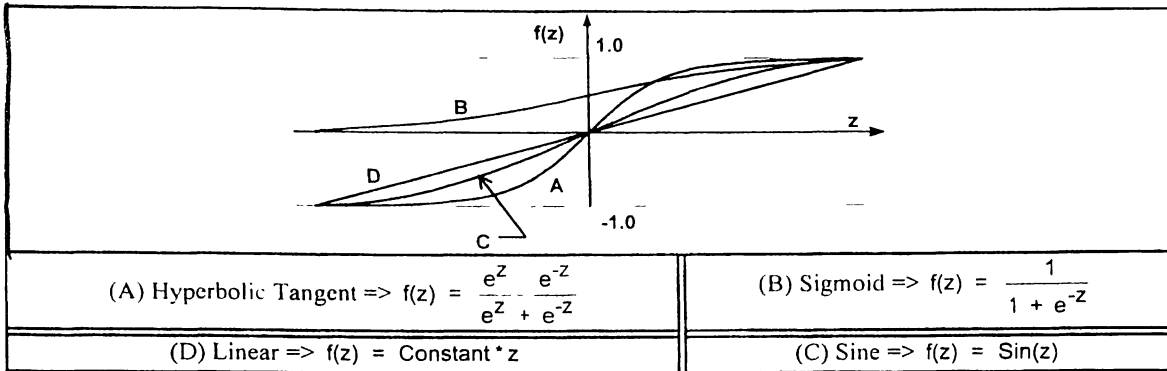


Figure 2.6 Transfer functions [9]

Processing elements are typically organized into groups called layers. In general, a network will consist of an input layer, one or more hidden layers, and an output layer. Data are presented to the network in the input layer, processing is accomplished in the hidden layers, and the response of the network is presented in the output layer. The architecture for a generic neural network is shown in Figure 2.7.

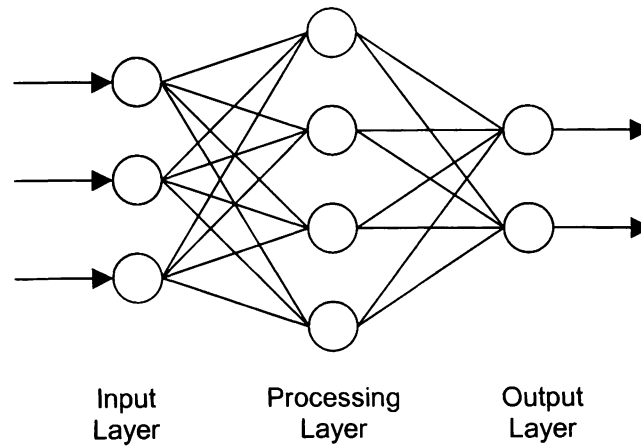


Figure 2.7 Generic neural network architecture

2.4.1 Backpropagation Neural Networks

A backpropagation neural network is a multilayered, supervised, feed forward network, as shown in Figure 2.8.

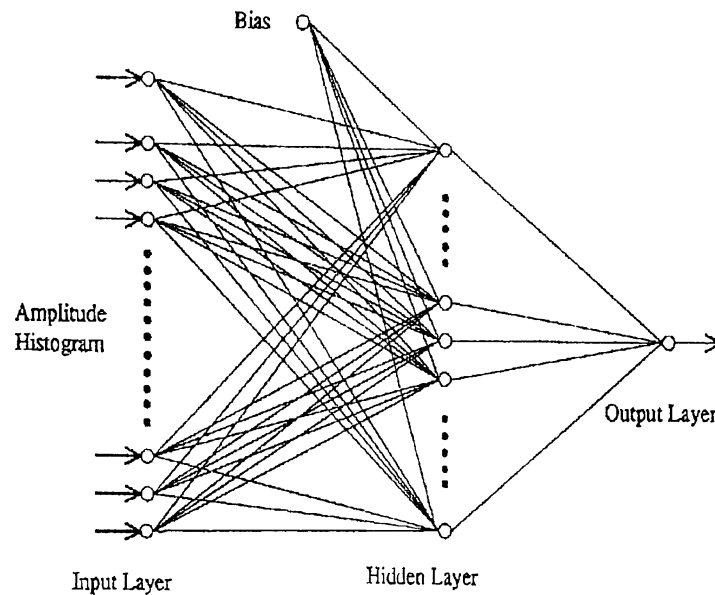


Figure 2.8 Backpropagation neural network

This type of network learns the relationship between the given input and the target output vector by minimizing the difference between the target and actual output vectors. The learning process consists of two stages. In the first stage, the input vectors are fed through the network to generate a response vector. In the second stage, the output error is computed for each input response based upon the target output values. The overall network error is then reduced by back propagating error adjustments to the network weights.

The algorithm for a simple backpropagation neural network is given by Walker and Hill [9]:

STAGE 1: Forward propagation of input vector

Step 1: Initialize weights to small random values

Step 2: Do while stopping condition is false

Step 3: Compute input sum and apply activation function for each middle PE:

$$y_j = f(w_{ij} * x_i)$$

Step 4: Compute input sum and apply activation function for each output PE:

$$z_k = f(v_{kj} * y_j)$$

STAGE 2: Back propagation of error

Step 5: Compute error: $\delta_k = (t_k - z_k) * f'(w_{jk} * y_j)$

Step 6: Compute delta weights: $\Delta v_{jk} = (\alpha)(\delta_k)(y_j) + \{\text{Momentum} * \Delta v_{jk}(\text{old})\}$

Step 7: Compute error contribution for each middle layer PE:

$$\delta_j = \delta_k * w_{jk} * f'(w_{ij} * x_i)$$

Step 8: Compute delta weights: $\Delta w_{ij} = (\alpha)(\delta_j)(x_i) + \{\text{Momentum} * \Delta w_{ij}(\text{old})\}$

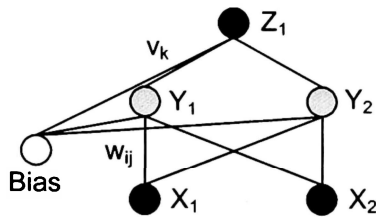
Step 9: Update weights: $Q_{rs}(\text{new}) = Q_{rs}(\text{old}) + \Delta Q_{rs}$

Step 10: Test stopping condition

Stopping conditions for a backpropagation neural network are when the weight changes have reached some minimal value or when the average error across a series of input vectors is below some desired level.

EXAMPLE

Consider a backpropagation network with 2 inputs and 2 hidden or middle layer PEs and a single output [9]. Find the new weights when the network is presented with an input vector $X_i = [0.0, 1.0]$ and target vector $Z_1 = 1.0$ using a learning coefficient of 0.25 and a sigmoid activation function.



The initial weights are given as:

$$w_{ij} = \begin{vmatrix} 0.7 & -0.4 & | & 0.4 \\ -0.2 & 0.3 & | & 0.6 \end{vmatrix}$$

$$v_k = \begin{vmatrix} 0.5 & 0.1 & | & -0.3 \end{vmatrix}$$

First compute the middle layer output using the relationship: $y_j = w_{ij} x_i$

$$y_1 = w_{11} x_1 + w_{21} x_2 + w_{1B} = (0.7)(0) + (-0.2)(1.0) + 0.4 = 0.2$$

$$y_2 = w_{12} x_1 + w_{22} x_2 + w_{2B} = (-0.4)(0) + (0.3)(1.0) + 0.6 = 0.9$$

$$y_{1(OUT)} = f(y_1) = 1 / (1 + e^{-y_1}) = 0.55$$

$$y_{2(OUT)} = f(y_2) = 1 / (1 + e^{-y_2}) = 0.71$$

Next, compute the network output and associated error using the relationship: $z_k = v_{ij} y_i$

$$z_1 = v_{11} y_1 + v_{12} y_2 + v_{1B} = (0.5)(0.55) + (0.1)(0.71) - 0.3 = 0.046$$

$$z_{1(OUT)} = f(z_1) = 1 / (1 + e^{-z_1}) = 0.51$$

$$\delta_k = (T_k - z_{k(OUT)}) f'(z_{k(OUT)})$$

$$\delta_{z_1} = (T_1 - z_{1(OUT)}) f(z_1)(1 - f(z_1)) = (1.0 - 0.51)(0.51)(1 - 0.51) = 0.12$$

The middle to output layer weights can now be updated using: $\Delta v_{jk} = \alpha \delta_k y_{j(\text{OUT})}$

$$\Delta v_{11} = \alpha \delta_{z1} y_{1(\text{OUT})} = (0.25)(0.12)(0.55) = 0.017$$

$$\Delta v_{12} = \alpha \delta_{z1} y_{2(\text{OUT})} = (0.25)(0.12)(0.71) = 0.021$$

$$\Delta v_{1B} = \alpha \delta_{z1} \text{Bias} = (0.25)(0.12)(1) = 0.030$$

$$v_k = | 0.517 \quad 0.121 \quad | \quad -0.270 \quad |$$

The second stage begins by computing the middle layer error as: $\delta_j = \delta_k v_{kj} f'(y_{j(\text{OUT})})$

$$\delta_{y1} = \delta_{z1} v_{11} f(y_1)(1 - f(y_1)) = (0.12)(0.5)(0.55)(1 - 0.55) = 0.015$$

$$\delta_{y2} = \delta_{z1} v_{12} f(y_2)(1 - f(y_2)) = (0.12)(0.1)(0.71)(1 - 0.71) = 0.0025$$

The input to middle layer weights are then updated using: $\Delta w_{ij} = \alpha \delta_i x_j$

$$\Delta w_{11} = \alpha \delta_{y1} x_1 = (0.25)(0.015)(0) = 0$$

$$\Delta w_{12} = \alpha \delta_{y1} x_2 = (0.25)(0.015)(1.0) = 0.0038$$

$$\Delta w_{21} = \alpha \delta_{y2} x_1 = (0.25)(0.0025)(0) = 0$$

$$\Delta w_{22} = \alpha \delta_{y2} x_2 = (0.25)(0.0025)(1.0) = 0.0006$$

$$\Delta w_{1B} = \alpha \delta_{y1} \text{Bias} = (0.25)(0.015)(1.0) = 0.0038$$

$$\Delta w_{2B} = \alpha \delta_{y2} \text{Bias} = (0.25)(0.0025)(1.0) = 0.0006$$

Finally, the new updated weights are given as:

$$w_{ij(\text{NEW})} = \left| \begin{array}{cc|c} 0.7 & -0.3962 & 0.4038 \\ -0.2 & 0.3006 & 0.6006 \end{array} \right|$$

This procedure can be repeated until the weight changes are no longer significant, at which point the network is considered to be trained.

2.4.2 Kohonen Self Organizing Maps

A Kohonen self organizing map (SOM) is a single layered, unsupervised, competitive neural network, as shown below.

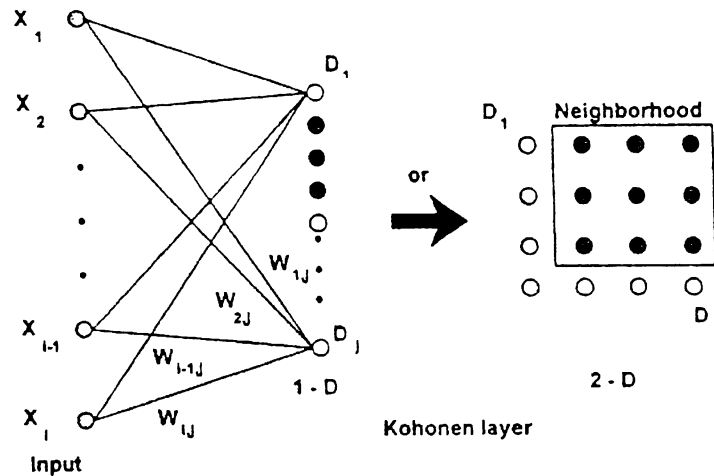


Figure 2.9 Kohonen self organizing map

A SOM is a neural network that sorts data into different categories, or creates a two-dimensional map from multi-dimensional inputs. When trained properly, a SOM can take data that is difficult to separate accurately, and divide it into different groups or clusters with common characteristics.

A SOM has an architecture that usually consists of an input layer and a two dimensional Kohonen layer. The processing elements in the input layer are not connected to each other, although, each processing element in the input layer is connected to all the processing elements in the Kohonen layer. Furthermore, the processing elements in the Kohonen layer are connected to each other. All of these connections have an associated weight.

A SOM learns by minimizing the Euclidean distance between the weights and the input vectors. The network attempts to cluster the input vectors on a mapping layer. The network not only clusters the input vectors but also locates groups with like behaviors close to each other. The algorithm for a simple Kohonen self organizing map is given by Walker and Hill [9]:

Step 1: Initialize weights, set neighborhood and learning rate parameters

Step 2: Do while stopping condition is false

Step 3: For each input vector, x_i

Step 4: Compute for each processing element: $D_j = \sum (w_{ij} - x_i)^2$

Step 5: Find index “j” for D_j minimum

Step 6: Update all weights in neighborhood of “j”

$$w_{ij(\text{NEW})} = w_{ij(\text{OLD})} + \alpha (x_i - w_{ij(\text{OLD})})$$

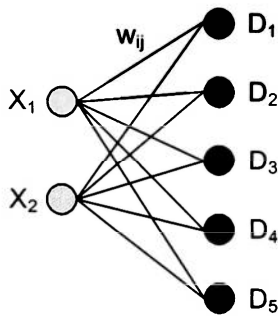
Step 7: Update learning rate and neighborhood parameters

Step 8: Test stopping condition

Typically, stopping conditions for a Kohonen self organizing map are when the network is said to have converged, or when the weight changes are small or after a sufficient number of training cycles are completed.

EXAMPLE

Consider a Kohonen self organizing network with 2 input processing elements and 5 cluster units [9]. Find the winning cluster unit for the input vector $x_i = [0.5, 0.2]$ and update network weights for one pass using a neighborhood factor of 1 and a learning coefficient of 0.2.



The initial weights are given as:

$$w_{ij} = \begin{vmatrix} 0.3 & 0.6 & 0.1 & 0.4 & 0.8 \\ 0.7 & 0.9 & 0.5 & 0.3 & 0.2 \end{vmatrix}$$

First the Euclidean distances are computed using: $D_j = \sum (w_{ij} - x_i)^2$

$$D_1 = (w_{11} - x_1)^2 + (w_{21} - x_2)^2 = (0.3 - 0.5)^2 + (0.7 - 0.2)^2 = 0.29$$

$$D_2 = (w_{12} - x_1)^2 + (w_{22} - x_2)^2 = (0.6 - 0.5)^2 + (0.9 - 0.2)^2 = 0.50$$

$$D_3 = (w_{13} - x_1)^2 + (w_{23} - x_2)^2 = (0.1 - 0.5)^2 + (0.5 - 0.2)^2 = 0.25$$

$$D_4 = (w_{14} - x_1)^2 + (w_{24} - x_2)^2 = (0.4 - 0.5)^2 + (0.3 - 0.2)^2 = \underline{0.02}$$

$$D_5 = (w_{15} - x_1)^2 + (w_{25} - x_2)^2 = (0.8 - 0.5)^2 + (0.2 - 0.2)^2 = 0.09$$

Since D_4 is the closest to zero it is deemed the winning processing element. With a neighborhood factor of 1, this implies that the weights for processing element “j” = 3, 4

and 5 will be updated using: $w_{ij(\text{NEW})} = w_{ij(\text{OLD})} + \alpha (x_i - w_{ij(\text{OLD})})$

$$w_{13(\text{NEW})} = w_{13(\text{OLD})} + \alpha (x_1 - w_{13(\text{OLD})}) = 0.1 + 0.2 (0.5 - 0.1) = 0.18$$

$$w_{23(\text{NEW})} = w_{23(\text{OLD})} + \alpha (x_2 - w_{23(\text{OLD})}) = 0.5 + 0.2 (0.2 - 0.5) = 0.44$$

$$w_{14(\text{NEW})} = w_{14(\text{OLD})} + \alpha (x_1 - w_{14(\text{OLD})}) = 0.4 + 0.2 (0.5 - 0.4) = 0.42$$

$$w_{24(\text{NEW})} = w_{24(\text{OLD})} + \alpha (x_2 - w_{24(\text{OLD})}) = 0.3 + 0.2 (0.2 - 0.3) = 0.28$$

$$w_{15(\text{NEW})} = w_{15(\text{OLD})} + \alpha (x_1 - w_{15(\text{OLD})}) = 0.8 + 0.2 (0.5 - 0.8) = 0.74$$

$$w_{25(\text{NEW})} = w_{25(\text{OLD})} + \alpha (x_2 - w_{25(\text{OLD})}) = 0.2 + 0.2 (0.2 - 0.2) = 0.20$$

Finally, the new weight matrix is given as:

$$w_{ij(\text{NEW})} = \begin{vmatrix} 0.3 & 0.6 & 0.18 & 0.42 & 0.74 \\ 0.7 & 0.9 & 0.44 & 0.28 & 0.20 \end{vmatrix}.$$

Again, this procedure can be repeated until the weight changes no longer affect the output.

CHAPTER 3

EXPERIMENTAL PROCEDURE

3.1 FIBERGLASS/EPOXY BEAMS

All of the fiberglass/epoxy beams used for testing were fabricated at Embry-Riddle Aeronautical University. Fifteen beams, measuring 381 mm in length, 36.6 mm in width, and 4.3 mm in thickness (15" x 1.4" x 0.17"), were fabricated using a wet layup with a room temperature cure.

Ren tooling was used for the fabrication of the beams (Figure 3.1). The ren tooling was cleaned with acetone and then treated with a paste wax release agent to prevent the adhesion of the beams to the tooling. The RO99-625 direct wind roving from Saint-Gobain Vetrotex America, Inc. was bundled into groups of seven rovings. Each bundle was approximately 137 cm (54 in) long and secured at one end with tape. Ten of these bundles laid out axially made up the 35.6 mm (1.4 in) width of each specimen.

West System 105 epoxy resin and West System 206 slow hardener were thoroughly mixed in a 5 to 1 ratio. The fiber bundles were completely wetted out by the epoxy resin, then fed through a metal die with a 4 mm (5/32 in) diameter hole to remove the excess resin and to ensure a constant fiber to resin ratio. The bundles were then laid one by one axially in the ren tool until all ten bundles were inside the tool. The fibers were then

pressed flat into the tool with a squeegee and left to cure at room temperature as shown below in Figure 3.1.

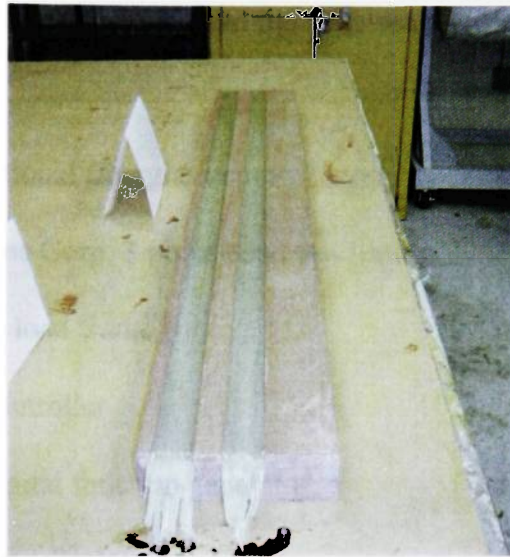
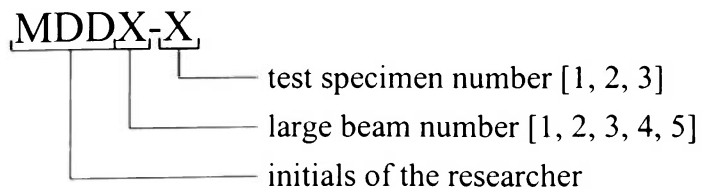


Figure 3.1 Beams curing at room temperature

After the beams were completely cured, a liquid cooled saw with a diamond coated blade was used to cut the 137 cm (54 in) beams into three 381 mm (15 in) long test specimens. Approximately 102 mm (4 in) of scrap were trimmed off of each end of the 137 cm (54 in) beams.

The 381 mm (15 in) test specimens were labeled according to the large beam and location they were cut from. Three test specimens were cut from each of the 5 large beams; hence, the numbers assigned to the large beams ranged from 1 through 5, and the numbers designated to the test specimens ranged from 1 through 3.

EXAMPLE



3.2 TEST SETUP

All 3-point bend testing was also performed at Embry-Riddle Aeronautical University.

The equipment used during testing included the following:

- 15 Unidirectional fiberglass/epoxy beams
- MTS Systems Corp. 3-point bend test fixture
- MTS 10 kip load frame
- MTS 407 controller
- MTS 410 digital function generator
- MTS 464 data display
- Physical Acoustics Corporation (PAC) laptop
- PAC μ DiSP/NB-8 data acquisition system
- 2 PAC R15I acoustic emission transducers
 - Channel 1 — S/N: F122
 - Channel 2 — S/N: FJ61
- Omega Engineering Inc. X-Y plotter
- BNC signal cables
- Sculpey III oven-bake clay
- Stanley hot melt glue gun
- Hot melt glue sticks
- 0.5 mm mechanical pencil with HB pencil lead

The complete test setup is shown in Figure 3.2, and the MTS setup is shown in Figure 3.3.

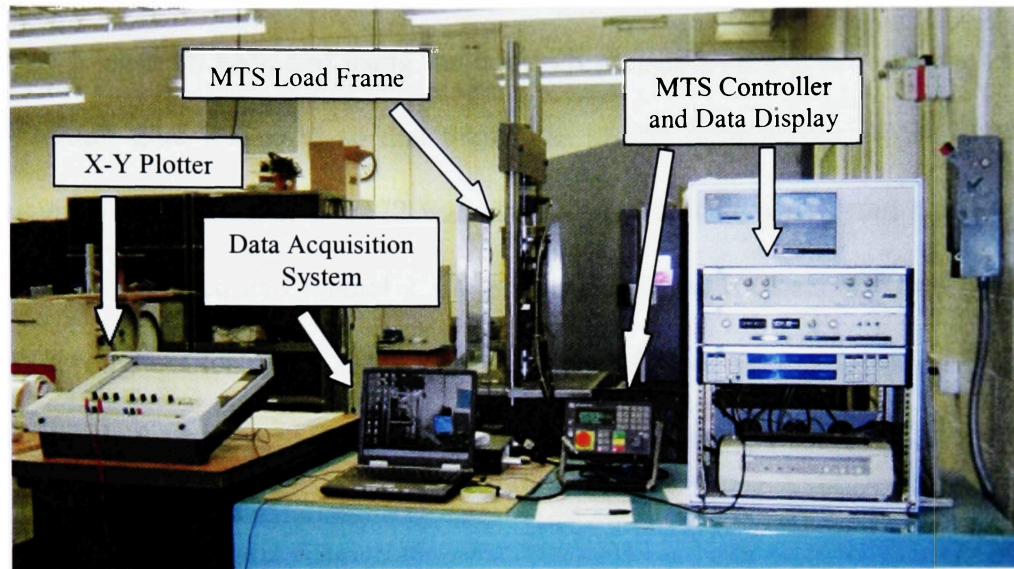


Figure 3.2 Complete test setup



Figure 3.3 MTS setup without beam specimen

3.2.1 Specimen Setup

Physical Acoustics Corporation R15I transducers were mounted onto the test specimens 38 mm (1.5 in) from each end using the hot melt glue as a couplant, as shown in Figure 3.4. (Enough glue was used so that there was visible squeeze out on all sides of the transducers.) Transducer S/N F122 was always used as Channel 1, and transducer S/N FJ61 was always used as Channel 2. The locations of both Channel 1 and 2 remained constant throughout testing. Channel 1 was on the left and Channel 2 was on the right as the observer is facing the MTS load frame. The transducers were connected to Channels 1 and 2 of the PAC data acquisition system.

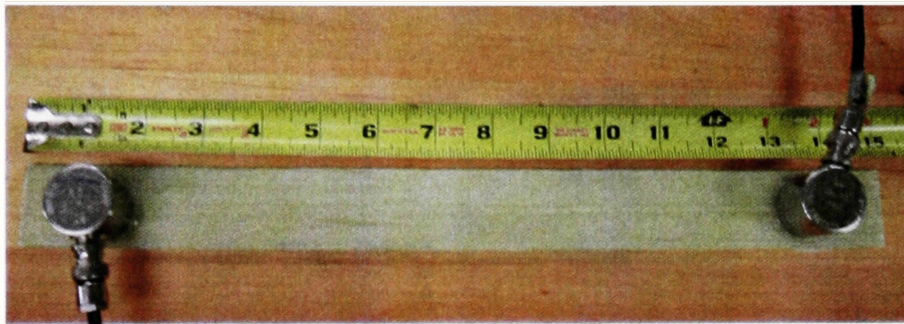


Figure 3.4 Transducers mounted on specimen

3.2.2 MTS Load Frame Setup

The 3-point bend test fixture was mounted in the hydraulic grips in the MTS machine. The span of the test fixture was set at 7 inches. Sculpey clay was applied to the 3 contact points on the test fixture to minimize any rubbing noise between the test fixture and the test specimen which could lead to unwanted AE data.

An X-Y plotter was connected to the load output from the MTS 407 controller to record load as a function of time. The data acquisition system also recorded the acoustic emission data as a function of time. Hence, if load is known as a function of time and the acoustic emission data is known as a function of time, then acoustic emission activity can be determined as a function of load.

3.3 DATA ACQUISITION

Data acquisition was accomplished using a PAC 4 channel data acquisition system. This was connected to a PAC laptop computer with PAC AEwin for DiSP software installed.

Pertinent setup parameters configured within the AEwin software are listed below:

- Preamp Gain: 40 dB
- Threshold: 40 dB
- Peak Detection Time (PDT): 40 μ s
- Hit Definition Time (HDT): 150 μ s
- Hit Lockout Time (HLT): 300 μ s

The setup parameters listed above were selected based on the recommendations of the PAC data acquisition user manual (Bibliography) for composite materials. The preamp gain is the amplification within the AE transducers. The PAC R15I transducers each have an integral preamplifier with a gain of 40 dB. The PDT is the maximum amount of time given for the system to detect the peak voltage of the AE waveform. If the PDT is set too high, the amplitude and the rise time parameters may be incorrect because the

system will mistakenly choose the wrong peak as the maximum. The HDT determines when one AE waveform ends and another begins. The HDT is the span of time spent after the AE waveform drops below the given threshold waiting to see if the waveform will rise above the threshold again. If the waveform does not rise above the threshold during the HDT, then it is considered over. If the HDT is set too high, the acquisition system will group several hits into one, causing multiple hit data. The HLT starts exactly when the HDT ends. The HLT is the time that it takes the acquisition system to move the collected data into its buffers.

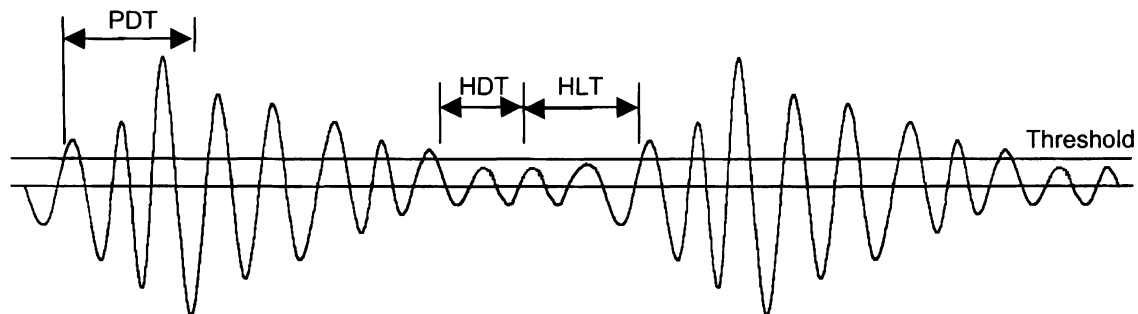


Figure 3.5 Waveform with setup parameters

3.4 TEST PROCEDURE

First, the test specimen was centered in the test fixture. The MTS crosshead was then adjusted so that the fixture was in contact with the test specimen without applying a load. The X-Y plotter and the data acquisition system were then started simultaneously while the MTS was ramped at a constant rate of 8.4 mm/min (0.33 in/min). The specimens were loaded to failure. Upon failure, the X-Y plotter and the data acquisition system were stopped. A test specimen in the test fixture prior to loading can be seen in Figure 3.6, and a specimen in the test fixture after failure is shown in Figure 3.7.

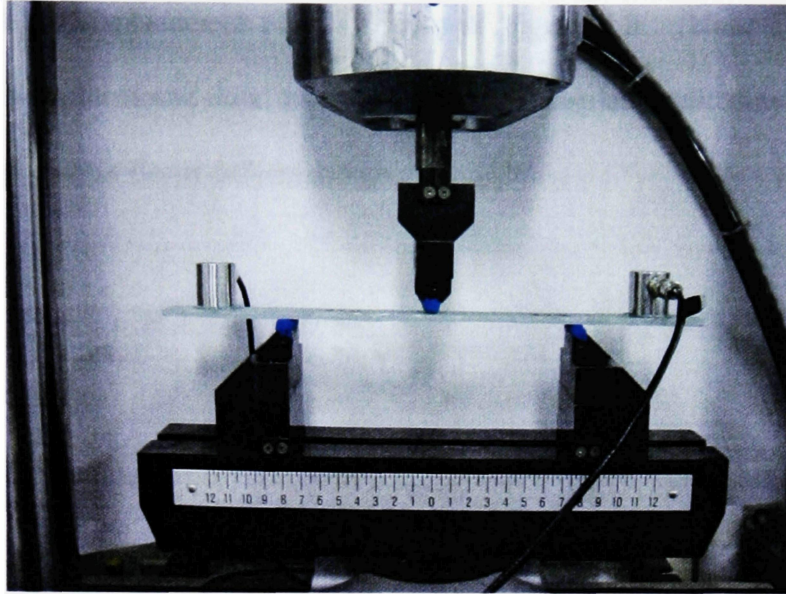


Figure 3.6 Test specimen prior to loading

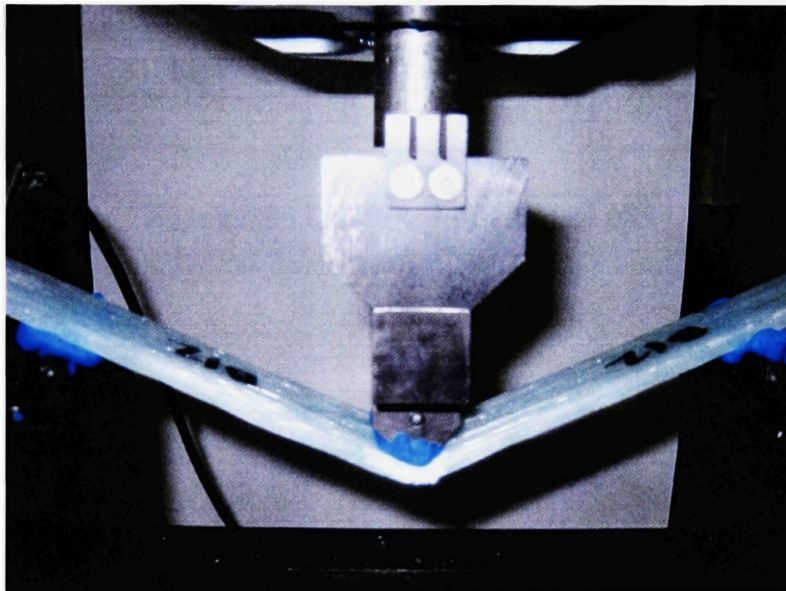


Figure 3.7 Test specimen after failure

A typical load vs. displacement plot is shown in Figure 3.8. (Note: The apparently compliant load-displacement data up to about 1 inch displacement may be due to clay deformation rather than beam deformation.)

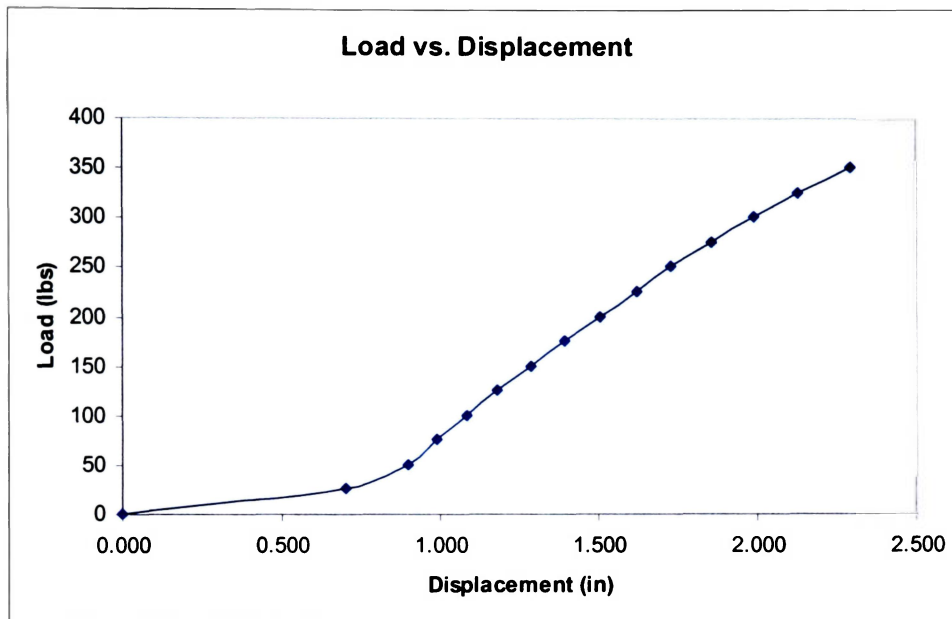


Figure 3.8 Load vs. displacement plot

CHAPTER 4

ANALYSIS AND RESULTS

4.1 ACOUSTIC EMISSION DATA

Acoustic emission data were collected from the onset of loading until failure for each of the 15 beam specimens. The ultimate load for each of the test specimens and total number of AE hits acquired are shown in Table 4.1. Using Chauvenet's criterion [10], no outliers were found among the ultimate loads.

Table 4.1 Ultimate loads and corresponding AE hits

Specimen ID	Ultimate Load (lbs)	Total Hits
MDD1-1	375	2757
MDD1-2	312.5	5509
MDD1-3	327.5	7901
MDD2-1	372.5	748
MDD2-2	365	1379
MDD2-3	357.5	3214
MDD3-1	336	1051
MDD3-2	312.5	820
MDD3-3	340	611
MDD4-1	363	2540
MDD4-2	372.5	1011
MDD4-3	392.5	1682
MDD5-1	367.5	1009
MDD5-2	375	1023
MDD5-3	365	2718
AVE	355.6	
STD	24.2	

The next step was to determine how much of the AE data would be required to make the desired ultimate load predictions. Fisher and Hill [4] were able to accurately predict burst pressures in fiberglass/epoxy filament wound composite pressure vessels using AE

data taken up to 25% of the expected burst pressure. Fatzinger and Hill [5] were able to predict the ultimate loads in fiberglass/epoxy I-beams using AE data taken up to 50% of the theoretical ultimate load. To determine how much to filter the data, the number of AE hits associated with the percentage of average ultimate load was needed (see Table 4.2). The number of hits associated with 75% of the average ultimate load was considered too sparse to use as the input to a backpropagation neural network. The network will not predict well using an amplitude distribution comprised of only 16 hits. Ninety percent and higher was not reasonable because specimens began failing at 312.5 lbs, which is less than 90% of the average ultimate load of 355.6 lbs; therefore, the neural network would be predicting on 100% of those specimens' AE data. The minimum number of hits associated with 80% and 85% were similar; however, 80% was chosen since the prediction should be made using the lowest possible proof load.

Table 4.2 AE hits associated with percentage of average ultimate load

Specimen ID	Percentage of Average Ultimate Load					
	75	80	85	90	95	100
MDD1-1	47	79	92	140	163	236
MDD1-2	148	210	326	5509	5509	5509
MDD1-3	97	109	280	805	7901	7901
MDD2-1	23	29	36	48	105	409
MDD2-2	114	154	191	244	400	619
MDD2-3	208	267	328	504	1154	1743
MDD3-1	16	32	41	101	1051	1051
MDD3-2	131	185	245	820	820	820
MDD3-3	48	64	86	127	274	611
MDD4-1	30	39	65	233	565	1099
MDD4-2	136	142	168	219	285	397
MDD4-3	60	106	138	214	316	435
MDD5-1	19	28	32	61	74	87
MDD5-2	22	29	37	52	138	273
MDD5-3	46	54	61	69	271	619

 indicates specimen failed and total AE data are included

Thus, the AE data were filtered to include only those data acquired up to 80% of the average ultimate load. A series of plots were then generated to graphically display correlations between the AE parameters. Appendix A contains the plots for all 15 test specimens. Figures 4.1, 4.2, and 4.3 show example AE plots for specimen MDD2-3.

The first step was to analyze the amplitude distribution plots. As mentioned previously, the amplitude distribution typically will exhibit humps that represent the various failure mechanisms. As seen in Figure 4.1, the failure mechanisms humps are blended together such that they cannot be readily distinguished because of the large number of hits (267).

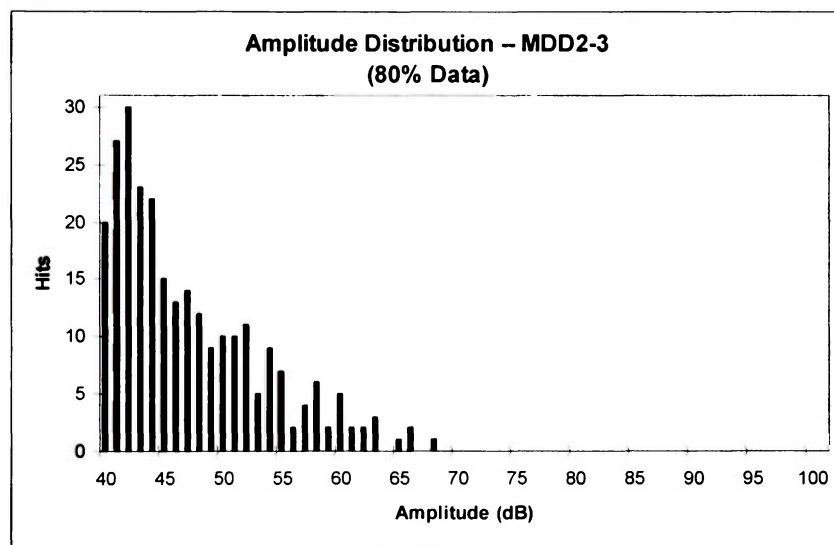


Figure 4.1 Amplitude distribution plot

The next step was to analyze the duration vs. amplitude plots. Typically, these plots show groups or clusters of hits that represent the failure mechanisms present [7]. As shown in Figure 4.2, there are no apparent groups or clusters present in the duration vs. amplitude plots either.

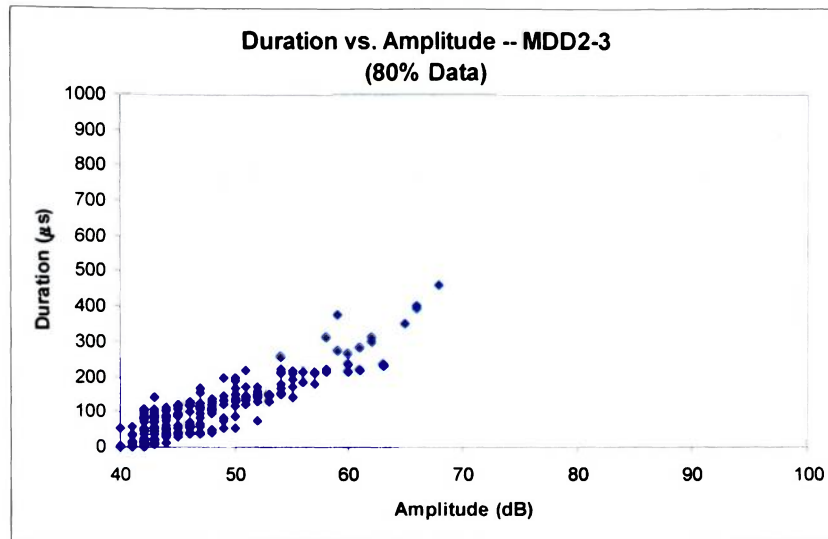


Figure 4.2 Duration vs. amplitude plot

The next step was to analyze the duration vs. counts plots. Typically, these plots show a linear relationship between the duration (D) of the AE waveform and the number of counts (C) for each hit ($D = kC$). If the plots show unusual scatter, this is an indication that there may be multiple hit data [7]. As shown in Figure 4.3, there is a linear relationship present in the duration vs. counts plots. Thus, the setup parameters (section 3.3) are probably correct, and multiple hit data are probably minimal. This is also indicated by the coefficient of determination, R^2 , being greater than 0.90.

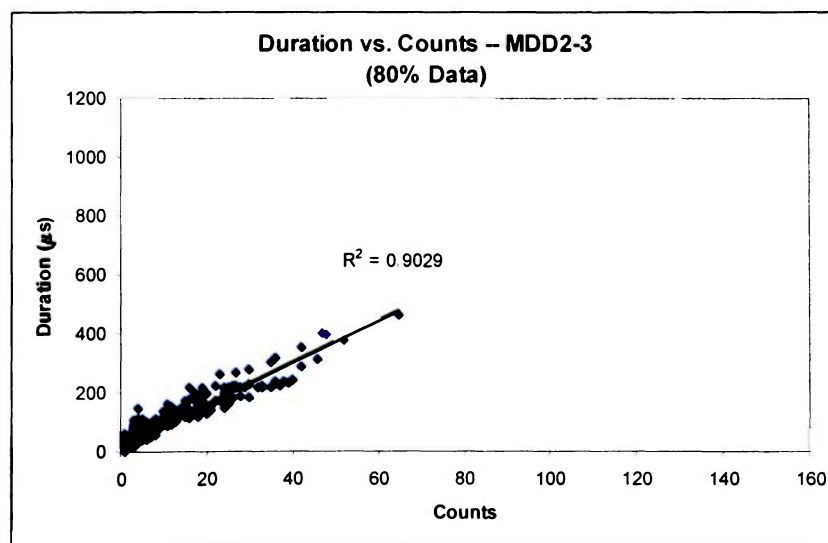


Figure 4.3 Duration vs. counts plot

4.2 BACKPROPAGATION NEURAL NETWORK

A series of backpropagation neural networks were optimized to predict the ultimate failure load using AE amplitude distribution data. Architecturally, each network consisted of a 61 neuron input layer for the amplitude hit frequencies, a hidden layer for mapping, and a 1 neuron output layer for predicting the ultimate load. NeuralWorks Professional II/Plus software by NeuralWare was used to create the neural networks.

Fifteen specimens were tested in all; each neural network was trained on 7 specimens and tested on the remaining 8 specimens. Because the networks were trained on the amplitude histograms from only 7 specimens, the data set was tripled to help the software learn on a larger set of data ($7 \times 3 = 21$ data sets). The randomized training and testing sets are shown in Tables 4.3 and 4.4, respectively. Note that the training set must include the high and low values of ultimate load in order to predict correctly [3].

Table 4.3 Training set

Specimen ID	Ultimate Load (lbs)	Amplitude Distribution Data
MDD3-1	336	3 9 6 2 4 2 0 0 1 0 2 0 0 0 1 0 0 1 0 1 0
MDD4-2	372.5	4 17 14 10 10 11 12 7 9 7 6 3 1 7 3 7 1 1 2 6 1 1 1 0 0 1 0
MDD2-3	357.5	20 27 30 23 22 15 13 14 12 9 10 10 11 5 9 7 2 4 6 2 5 2 2 3 0 1 2 0 1 0
MDD1-2	312.5	14 18 18 9 12 9 10 14 15 11 5 14 12 5 1 4 8 1 3 2 2 2 2 4 1 0 3 3 3 1 2 0 1 0 0 1 0
MDD4-3	392.5	7 10 9 7 8 2 5 3 1 4 2 1 2 2 2 3 4 4 3 4 1 3 4 5 0 2 0 0 2 0 1 2 1 1 1 0
MDD5-2	375	2 2 4 3 2 2 1 2 1 3 1 1 2 0 1 0 0 1 0 1 0
MDD5-3	365	4 12 7 6 5 3 1 2 3 1 1 0 0 1 1 0 1 1 0 1 3 0 0 0 0 1 0

Table 4.4 Testing set

Specimen ID	Ultimate Load (lbs)	Amplitude Distribution Data
MDD1-1	375	6 9 10 2 9 4 4 4 2 3 4 3 1 2 1 2 1 2 1 2 2 3 1 0 1 0
MDD3-2	312.5	14 19 24 13 16 12 9 5 4 6 5 2 4 9 3 5 4 7 4 2 3 2 3 2 3 0 0 0 0 1 0 0 0 0 1 0 1 2 0
MDD2-2	365	5 11 15 8 9 8 5 9 7 6 1 0 3 3 3 4 4 4 3 3 3 4 5 5 2 3 4 2 3 2 2 2 1 2 1 1 0 0 0 1 0
MDD1-3	327.5	9 15 8 14 10 12 9 3 5 5 3 5 2 1 1 1 2 1 1 0 1 1 0
MDD3-3	340	3 14 11 6 7 7 7 1 1 0 0 1 0 2 0 0 1 0 1 0 0 1 1 0
MDD4-1	363	3 4 7 5 3 5 3 1 2 0 1 0 0 0 0 1 0 0 0 0 0 0 1 0 0 1 2 0
MDD2-1	372.5	1 3 4 2 4 1 1 0 1 3 2 0 1 0 0 0 0 0 1 2 3 0
MDD5-1	367.5	0 5 2 1 2 1 1 0 1 1 0 1 2 1 0 1 1 2 1 0 1 2 0 0 0 1 1 0

The first backpropagation neural network was generated using the parameters as shown in Table 4.5. Based on previous research, the normalized-cumulative-delta rule (for further explanation, see Appendix B under **Learn Rule**) was used as the learning rule, and the hyperbolic tangent was used as the transfer function. The epoch size was set to be twenty-one or the size of the training file repeated three times in random order. The network was trained until the RMS error converged to 3%. The remaining parameter values were the software defaults and were varied subsequently to obtain the optimum values. (For a complete list of definitions of the network parameters see Appendix B.)

Table 4.5 Network parameters

Network Number	1
Inputs	61
Hidden 1	2
Output	1
L. Coef.	0.3
	0.15
Momentum	0.4
Trans. Pt.	10000
L. Coef. Ratio	0.5
F' Offset	0.1
Learn Rule	NCD
Transfer	tanH
Epoch	21
RMS Error	0.03

The first parameter that was optimized was the number of PEs in the hidden layer. The results are summarized in Figure 4.4. For the complete results from all network permutations, see Appendix C.

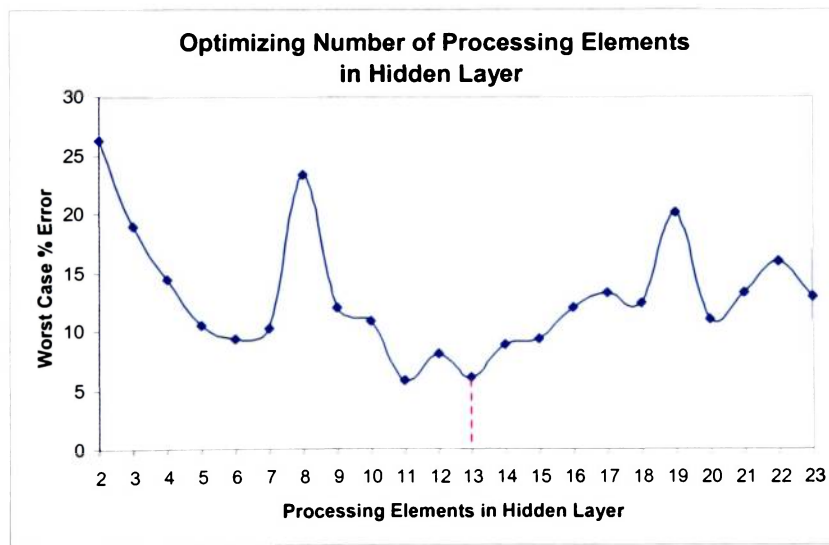


Figure 4.4 Optimizing number of processing elements in hidden layer plot

After the optimum number of PEs in the hidden layer was determined to be 13, that parameter and all other parameters were fixed while the F' offset was varied. The results are displayed in Figure 4.5.

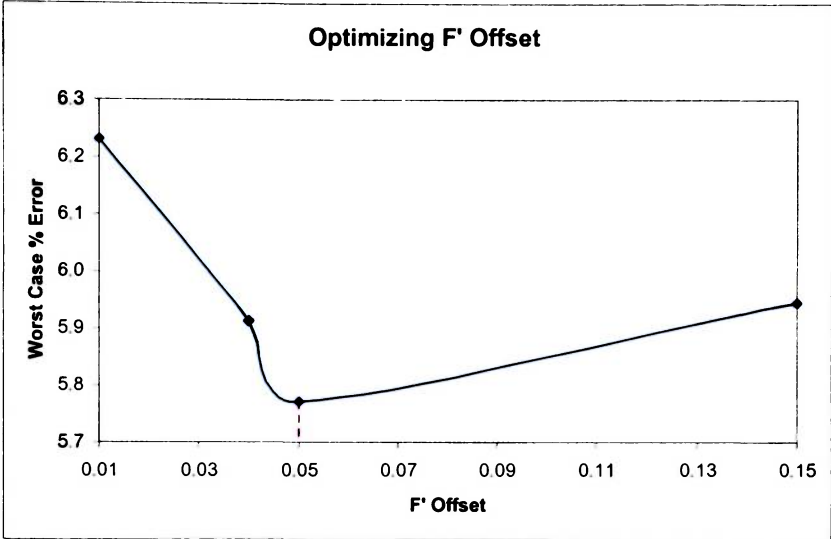


Figure 4.5 Optimizing F' offset plot

The above optimization procedure was repeated for the remainder of the network parameters. These results are shown in Figures 4.6 through 4.11 and summarized in Table 4.6.

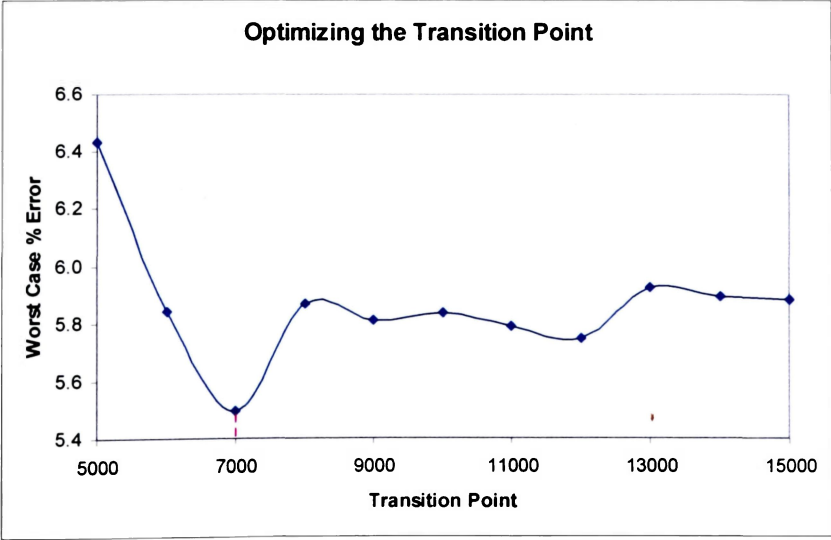


Figure 4.6 Optimizing transition point plot

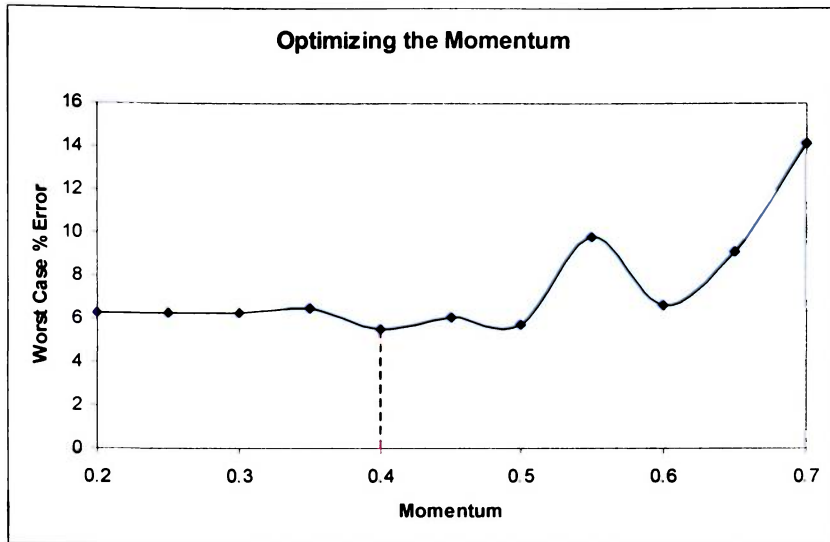


Figure 4.7 Optimizing the momentum plot

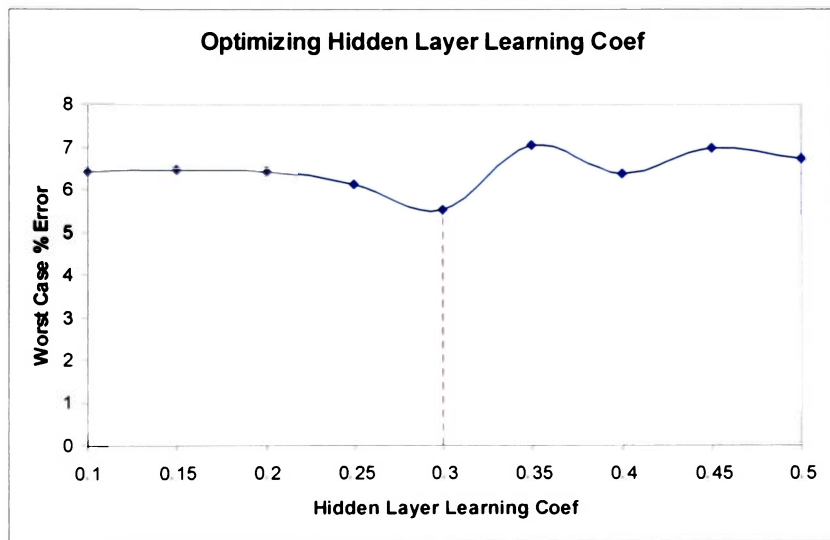


Figure 4.8 Optimizing hidden layer learning coefficient plot

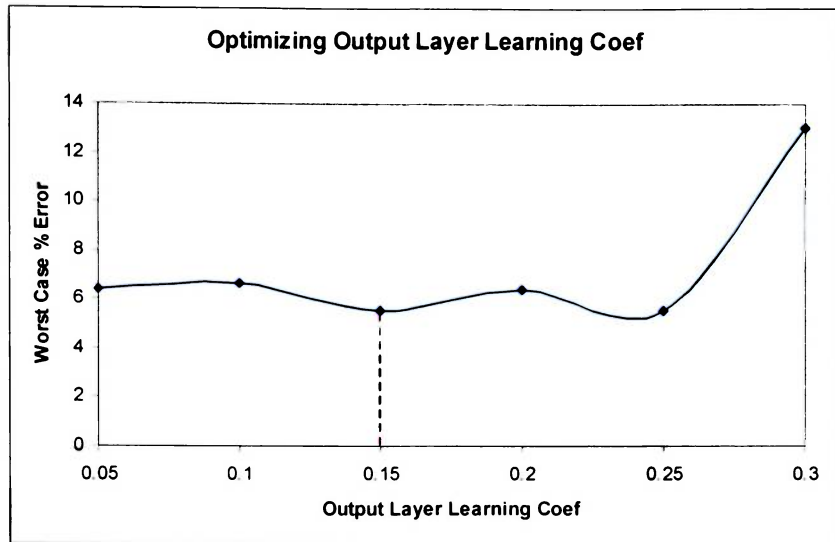


Figure 4.9 Optimizing output layer learning coefficient plot

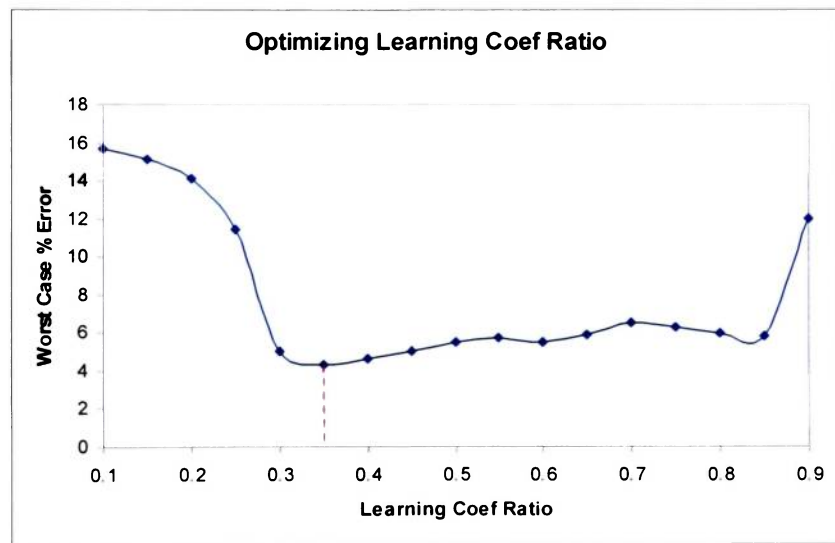


Figure 4.10 Optimizing learning coefficient ratio plot

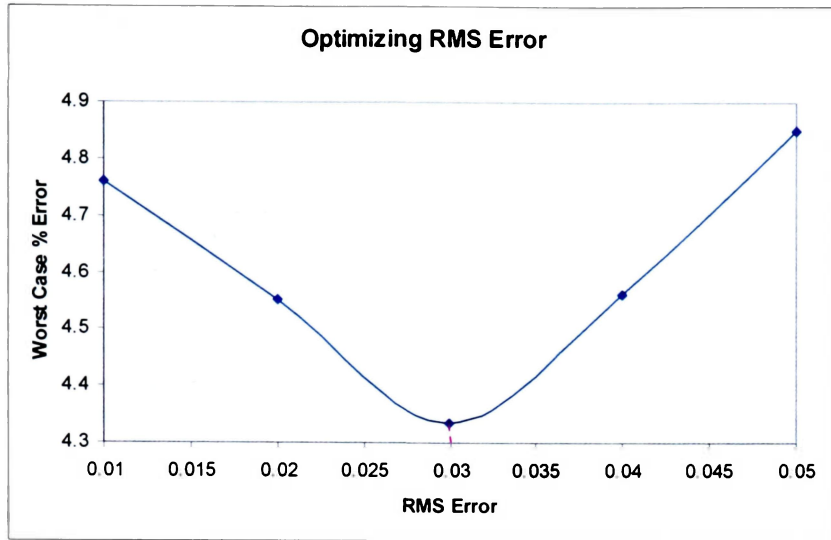


Figure 4.11 Optimizing RMS error plot

Table 4.6 Final network parameters

Network Number	82
Inputs	61
Hidden 1	13
Output	1
L. Coef.	0.3
	0.15
Momentum	0.4
Trans. Pt.	7000
L. Coef. Ratio	0.35
F' Offset	0.05
Learn Rule	NCD
Transfer	tanH
Epoch	21
RMS Error	0.03

Using the optimized network parameters, the resulting backpropagation neural network ultimate load predictions are summarized in Table 4.7. As can be seen (highlighted), the backpropagation neural network was able to predict the ultimate loads with a worst case error of 4.34 percent, which is within the desired goal of ± 5 percent.

Table 4.7 Backpropagation neural network results

	Specimen ID	Actual Load (lbs)	Predicted Load (lbs)	% Error
Training Data	MDD3-1	336	333.6	-0.72
	MDD4-2	372.5	372.5	-0.01
	MDD2-3	357.5	357.6	0.03
	MDD1-2	312.5	312.0	-0.16
	MDD4-3	392.5	392.7	0.06
	MDD5-2	375	378.1	0.83
	MDD5-3	365	364.9	-0.02
Test Data	MDD1-1	375	359.4	-4.15
	MDD3-2	312.5	326.0	4.34
	MDD2-2	365	354.2	-2.97
	MDD1-3	327.5	334.5	2.14
	MDD3-3	340	325.5	-4.26
	MDD4-1	363	361.9	-0.31
	MDD2-1	372.5	378.8	1.69
	MDD5-1	367.5	383.1	4.25

4.3 KOHONEN SELF ORGANIZING MAP

A series of Kohonen self organizing maps (SOMs) were generated to classify the AE parameter data (energy, duration, and amplitude) into failure mechanisms. The first step was to create a large enough SOM such that each failure mechanism would be sorted into its own category. A 20 x 20 SOM was chosen because it can sort the data into 400 possible categories. Architecturally, the SOM consisted of a 3 neuron input layer for energy, duration and amplitude, a 20 x 20 Kohonen layer for processing, and a 2 neuron output layer for X-Y (2-D) output coordinates. The 20 x 20 SOM was generated using the parameters shown in Table 4.8. NeuralWorks Professional II/Plus software by NeuralWare was used to construct the neural networks. (For a complete list of definitions of the network parameters see Appendix B.)

Table 4.8 20 x 20 SOM network parameters

Inputs	3
Rows	20
Columns	20
L. Coef.	0.06
SOM Steps	101730
Gamma	1
L. Coef. Ratio	0.5
Trans. Pt.	10000
Learn Rule	NCD
Transfer	tanH
Coord. Layer	Yes
Min-Max	Yes
Neighborhood	Square
Start Width	1
End Width	1
Epoch	3391

The SOM was trained using the AE data acquired from the onset of loading until failure for each of the 15 test specimens. Due to the extremely large quantity of data, the training file was filtered to contain only every 10th data hit. Upon completion of training, testing files were created for each of the 15 test specimens. All 15 test files were run through the 20 x 20 SOM, and the results were compiled into one file. The output file contained an X-Y coordinate associated with every data hit. The data vectors were then sorted into failure mechanisms based on their X-Y coordinates. Subsequently, the range, mean, standard deviation and number of hits associated with each failure mechanism were determined for the three AE parameters (energy, duration, and amplitude). The results for the 20 x 20 SOM are shown in Figure 4.12 and Table 4.9.

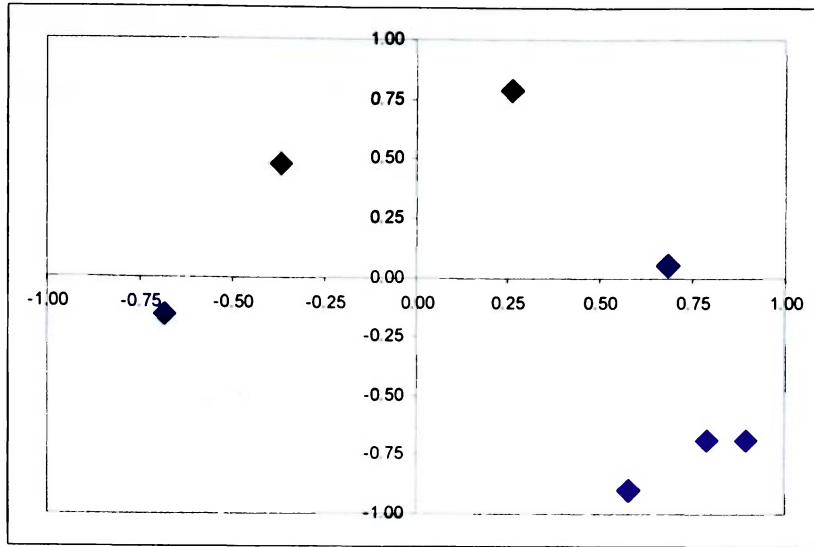


Figure 4.12 X-Y coordinate plot

Table 4.9 20 x 20 SOM results for energy, duration, and amplitude

Energy							
Mechanism	X	Y	Min	Max	Mean	STD	# of Hits
1	0.8947	-0.6842	0	8	0	0	20661
2	0.7895	-0.6842	0	40	2	2	9983
3	-0.3684	0.4737	2	264	18	24	3249
4	0.5789	-0.8947	141	2475	551	449	65
5	-0.6842	-0.1579	2647	2647	2647	0	1
6	0.6842	0.0526	1055	1055	1055	0	1
7	0.2632	0.7895	167	646	340	166	13
Duration							
Mechanism	X	Y	Min	Max	Mean	STD	# of Hits
1	0.8947	-0.6842	1	1375	45	57	20661
2	0.7895	-0.6842	8	3858	186	183	9983
3	-0.3684	0.4737	115	7864	555	722	3249
4	0.5789	-0.8947	989	11996	2908	2481	65
5	-0.6842	-0.1579	26597	26597	26597	0	1
6	0.6842	0.0526	29367	29367	29367	0	1
7	0.2632	0.7895	7469	15456	10599	2991	13
Amplitude							
Mechanism	X	Y	Min	Max	Mean	STD	# of Hits
1	0.8947	-0.6842	40	46	43	2	20661
2	0.7895	-0.6842	47	56	50	3	9983
3	-0.3684	0.4737	57	84	63	5	3249
4	0.5789	-0.8947	81	99	91	6	65
5	-0.6842	-0.1579	98	98	98	0	1
6	0.6842	0.0526	82	82	82	0	1
7	0.2632	0.7895	61	79	70	6	13

Figure 4.12 shows that the 20 x 20 SOM classified the input data into 7 failure mechanisms. From Table 4.9, it can be seen that mechanisms 1, 2 and 3 contain a large number of hits compared to mechanisms 4, 5, 6 and 7. Also, while the max and min ranges of amplitude for mechanisms 1, 2 and 3 do not overlap, the max and min ranges for mechanisms 4, 5, 6 and 7 do overlap. Therefore, it was thought that it might be possible to combine mechanisms 4, 5, 6 and 7 such that the total number of mechanisms would be either 4 or 5 instead of 7.

Thus, the next step was to generate a 5 x 1 SOM in order to force the data into 5 categories. The 5 x 1 SOM used the exact same testing and training files as the 20 x 20 SOM. The network parameters for the 5 x 1 SOM are shown in Table 4.10.

Table 4.10 5 x 1 SOM network parameters

Inputs	3
Rows	5
Columns	1
L. Coef.	0.06
SOM Steps	101730
Gamma	1
L. Coef. Ratio	0.5
Trans. Pt.	10000
Learn Rule	NCD
Transfer	tanH
Coord. Layer	Yes
Min-Max	Yes
Neighborhood	Square
Start Width	1
End Width	1
Epoch	3391

The 5 x 1 SOM was trained using the same procedure as used for the 20 x 20 SOM. The results for the 5 x 1 SOM are listed in Table 4.11.

Table 4.11 5 x 1 SOM results for energy, duration, and amplitude

Energy							
Mechanism	X	Y	Min	Max	Mean	STD	# of Hits
1	0	-0.5	0	8	0	0	20661
2	0	0.5	0	40	2	2	9983
3	0	1	2	353	19	27	3258
4	0	-1	514	2647	989	838	6
5	0	0	141	2475	551	449	65
Duration							
Mechanism	X	Y	Min	Max	Mean	STD	# of Hits
1	0	-0.5	1	1375	45	57	20661
2	0	0.5	8	3858	186	183	9983
3	0	1	115	11913	578	844	3258
4	0	-1	13888	29367	19052	6996	6
5	0	0	989	11996	2908	2481	65
Amplitude							
Mechanism	X	Y	Min	Max	Mean	STD	# of Hits
1	0	-0.5	40	46	43	2	20661
2	0	0.5	47	56	50	3	9983
3	0	1	57	84	63	5	3258
4	0	-1	69	98	80	10	6
5	0	0	81	99	91	6	65

Notice that the 5 x 1 SOM did force the data into 5 mechanisms. Mechanisms 1, 2 and 3 still contained a large number of hits compared to mechanisms 4 and 5. The max and min ranges of amplitude for mechanisms 1, 2 and 3 do not overlap; however, the max and min ranges for mechanisms 4 and 5 do overlap. Therefore, it was decided to combine mechanisms 4 and 5. This required the generation of a 4 x 1 SOM to force the data into 4 categories instead of 5. Again, the 4 x 1 SOM used the exact same testing and training files as the 20 x 20 SOM. The network parameters for the 4 x 1 SOM are shown in Table 4.12.

Table 4.12 4 x 1 SOM network parameters

Inputs	3
Rows	4
Columns	1
L. Coef.	0.06
SOM Steps	101730
Gamma	1
L. Coef. Ratio	0.5
Trans. Pt.	10000
Learn Rule	NCD
Transfer	tanH
Coord. Layer	Yes
Min-Max	Yes
Neighborhood	Square
Start Width	1
End Width	1
Epoch	3391

Once again, the 4 x 1 SOM was trained using the same procedure as used for the 20 x 20 SOM. The results for the 4 x 1 SOM are summarized in Table 4.13.

Table 4.13 4 x 1 SOM results for energy, duration, and amplitude

Energy							
Mechanism	X	Y	Min	Max	Mean	STD	# of Hits
1	0	-1	0	3	0.02	0.18	16232
2	0	-0.3	0	16	0.74	0.96	10374
3	0	0.3	0	90	4.5	4.7	5633
4	0	1	4	2647	52	153	1734
Duration							
Mechanism	X	Y	Min	Max	Mean	STD	# of Hits
1	0	-1	1	569	32	43	16232
2	0	-0.3	4	1779	119	103	10374
3	0	0.3	40	7864	295	322	5633
4	0	1	162	29367	891	1666	1734
Amplitude							
Mechanism	X	Y	Min	Max	Mean	STD	# of Hits
1	0	-1	40	44	42	1.3	16232
2	0	-0.3	45	50	47	1.7	10374
3	0	0.3	51	61	55	3.0	5633
4	0	1	60	99	68	6.7	1734

Here it is seen that the 4 x 1 SOM forced the data into 4 mechanisms, which agrees with the work of Graham [11]. The max and min ranges of the amplitude only slightly overlap for mechanisms 3 and 4. The sorted data for specimen MDD2-3 can be seen graphically in Figure 4.13. Here the scattered data above the trend line are multiple hits.

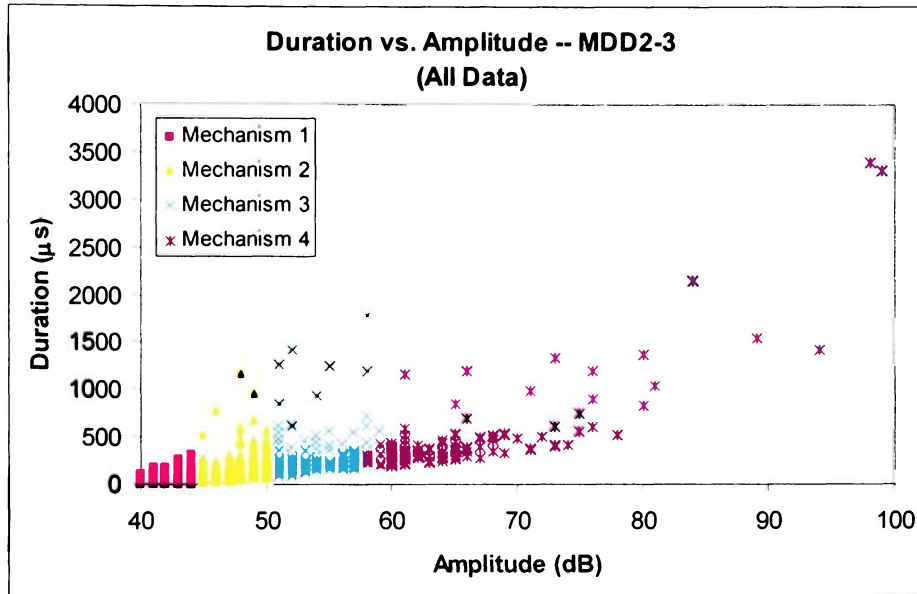


Figure 4.13 Sorted duration vs. amplitude plot

Amplitude distribution plots were generated to show how the 4 x 1 SOM classified the failure mechanisms. Figure 4.14 shows the amplitude distribution for all the data acquired for all 15 specimens. Here the failure mechanism ranges are clearly defined with the exception of mechanisms 3 and 4 overlapping slightly.

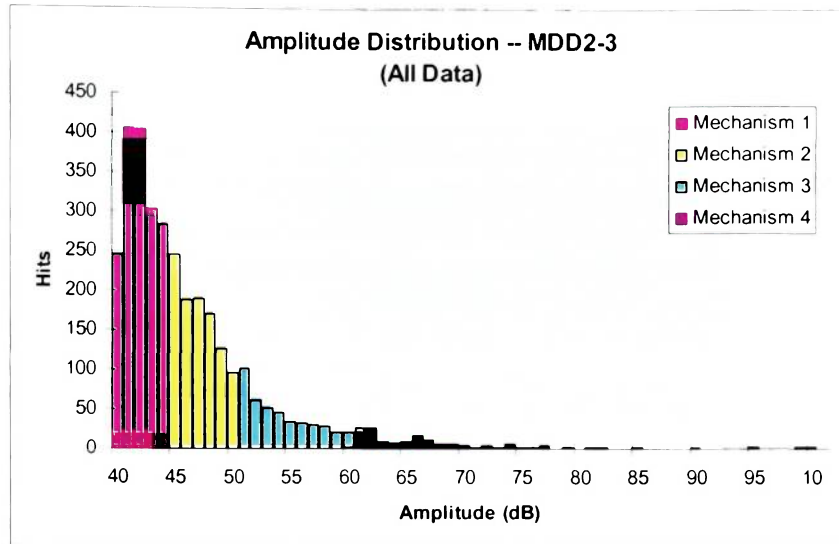


Figure 4.14 Sorted amplitude distribution plot

Through visual inspection of the beam specimens, it was seen that transverse matrix cracking, delaminations, fiber breaks and longitudinal matrix cracking (fiber/matrix debonding) were all present. Mechanism 1 had a low amplitude range (40-44 dB), a short duration range (1-569 μs) and a low energy range (0-3). Mechanism 2 had a low amplitude range (45-50 dB), medium short to medium durations (4-1,779 μs), and a low energy range (0-16). Mechanism 3 had a medium amplitude range (51-61 dB), medium durations (40-7,864 μs), and a medium energy range (0-90). Mechanism 4 has a high amplitude range (60-99 dB), a long duration (162-29,367 μs), and a high energy range (4-2,647). In addition, from comparison of the duration vs. amplitude plots containing 100% of the data and the plots filtered to 80% (Figure 4.15), most of the data hits in mechanisms 3 and 4 are not present in the 80% plots. Multiple hits are typically most prevalent during final failure; hence, if failure is eliminated from the data, it would be expected that multiple hits would be eliminated as well.

A second 4 x 1 SOM was generated to classify the AE data taken up to 80% of the average ultimate load. The 4 x 1 SOM was trained using the same procedure as used for the 20 x 20 SOM. Upon completion of training, all 15 test files were again run through the SOM and the results compiled into one file. The output file contained an X-Y coordinate associated with every data hit. The data vectors were then distributed into failure mechanisms based on same X-Y coordinates. From this, the range, mean, standard deviation and number of hits associated with each failure mechanism were determined for each AE parameter. The results for the 4 x 1 SOM are listed in Table 4.14.

Table 4.14 4 x 1 SOM results for 80% data

Energy							
Mechanism	X	Y	Min	Max	Mean	STD	# of Hits
1	0	-1	0	1	0	0.04	608
2	0	-0.3	0	2	0.5	0.55	465
3	0	0.3	1	8	3.5	1.76	328
4	0	1	6	78	16.9	12.3	121
Duration							
Mechanism	X	Y	Min	Max	Mean	STD	# of Hits
1	0	-1	1	125	25	27.2	608
2	0	-0.3	19	217	93	34.5	465
3	0	0.3	80	333	200	48.2	328
4	0	1	229	924	388	130.8	121
Amplitude							
Mechanism	X	Y	Min	Max	Mean	STD	# of Hits
1	0	-1	40	45	42	1.3	608
2	0	-0.3	43	52	47	2.0	465
3	0	0.3	49	62	55	3.2	328
4	0	1	59	79	66	4.4	121

Here it is seen that the 4 x 1 SOM forced the data into 4 mechanisms, again consistent with the results obtained by Graham [11]. The max and min ranges of the amplitude slightly overlap for all mechanisms, as they should. The sorted data for specimen MDD2-3 can be seen in Figure 4.15. Comparing Figure 4.15 with Figure 4.13, it can be

seen that almost all of the multiple hit data are eliminated by taking the load to only 80% of failure, plus mechanisms 3 and 4 are greatly reduced.

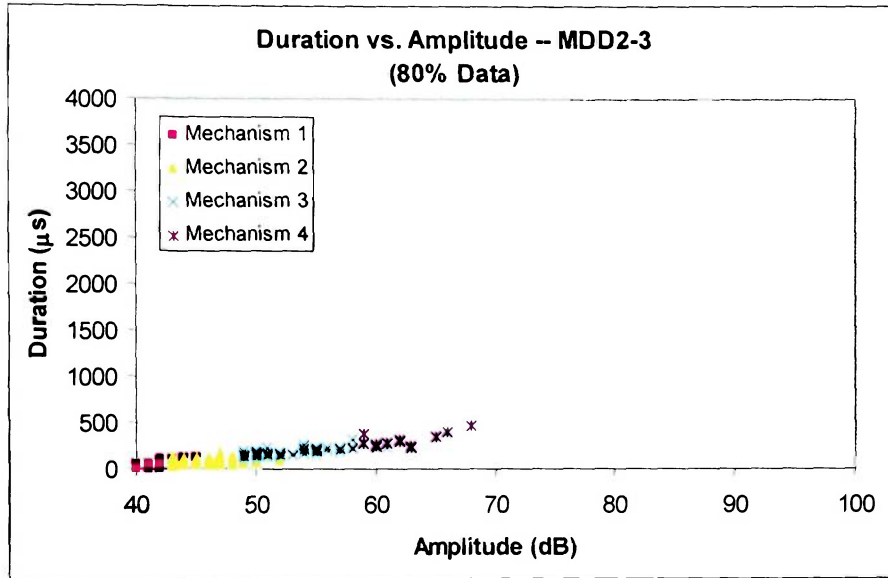


Figure 4.15 Sorted duration vs. amplitude plot for 80% data

4.4 MULTIVARIATE STATISTICAL ANALYSIS

After categorizing the 80% AE data into failure mechanisms, multivariate statistical analysis was performed to determine a prediction equation based on the number of hits in each of the failure mechanism categories. Statgraphics Plus was the program used to calculate the coefficients of the prediction equation. The dependent variable was the ultimate load and the four independent variables were the number of hits per failure mechanism for each specimen. The inputs to the analysis software are given in Table 4.15.

Table 4.15 Multiple linear regression inputs

Specimen ID	Number of Hits per Mechanism				Actual Load (lbs)
	Mechanism 1	Mechanism 2	Mechanism 3	Mechanism 4	
MDD1-1	33	24	18	4	375
MDD1-2	62	72	56	20	312.5
MDD1-3	51	41	16	1	327.5
MDD2-1	12	9	7	1	372.5
MDD2-2	45	40	31	38	365
MDD2-3	108	85	63	11	357.5
MDD3-1	24	4	4	0	336
MDD3-2	77	45	43	15	312.5
MDD3-3	40	18	5	1	340
MDD4-1	21	13	2	3	363
MDD4-2	51	57	32	2	372.5
MDD4-3	34	25	26	21	392.5
MDD5-1	9	5	11	3	367.5
MDD5-2	10	13	6	0	375
MDD5-3	31	14	8	1	365

The multiple linear regression (MLR) analysis produced the following prediction equation:

$$\text{Predicted Load} = 372.96 - 0.687 * (\text{Mech 1}) + 0.214 * (\text{Mech 2}) + 0.107 * (\text{Mech 3}) + 0.188 * (\text{Mech 4}).$$

Using the equation produced by the MLR analysis, the ultimate load was predicted for each specimen using the number of hits per failure mechanism as the variables. The best results were produced when predicting on failure mechanisms 1 and 2 only. Thus, the prediction equation became the following:

$$\text{Predicted Load} = 372.96 - 0.687 * (\text{Mech 1}) + 0.214 * (\text{Mech 2}).$$

The results of the prediction equation can be seen in Table 4.16. The worst case prediction error was -11.34 percent, which was outside the desired $\pm 5\%$ worst case error goal.

Table 4.16 Multiple linear regression analysis results

Specimen ID	Actual Load (lbs)	Predicted Load (lbs)	% Error
MDD1-1	375	355.4	-5.22
MDD1-2	312.5	345.8	10.65
MDD1-3	327.5	346.7	5.86
MDD2-1	372.5	366.6	-1.57
MDD2-2	365	350.6	-3.94
MDD2-3	357.5	317.0	-11.34
MDD3-1	336	357.3	6.35
MDD3-2	312.5	329.7	5.50
MDD3-3	340	349.3	2.74
MDD4-1	363	361.3	-0.46
MDD4-2	372.5	350.1	-6.01
MDD4-3	392.5	355.0	-9.57
MDD5-1	367.5	367.8	0.09
MDD5-2	375	368.9	-1.63
MDD5-3	365	354.7	-2.83

CHAPTER 5

CONCLUSIONS AND RECOMMENDATIONS

5.1 CONCLUSIONS

- The Kohonen self organizing map appeared to successfully classify the AE data into 4 failure mechanisms. Duration, energy and amplitude data were the only AE parameters used for classification.
- The backpropagation neural network successfully predicted the ultimate loads in unidirectional fiberglass/epoxy beams subjected to 3-point bending from the acoustic emission amplitude data taken up to 80% of the average ultimate load within the desired ± 5 percent goal.
- Multivariate statistical analysis using the number of hits associated with each failure mechanism predicted ultimate failure loads, but not within the desired goal of ± 5 percent.
- The backpropagation neural network probably provided better prediction results than the multivariate statistical analysis because multivariate statistical analyses are inherently sensitive to noisy (multiple hit) or sparse data, whereas backpropagation neural networks are not.

5.2 RECOMMENDATIONS

- Some multiple hit data were acquired during testing mostly at or near failure. The hit lockout time (HLT) and hit definition time (HDT) might be lowered to reduce multiple hit data.
- The failure mechanisms present were assumed to be transverse matrix cracking, longitudinal matrix cracking, fiber breaks and delaminations. The failure mechanisms should be verified using microscopic failure analysis on all of the test specimens.
- The use of broadband transducers for frequency analysis may improve failure mechanism classification.
- No simulated manufacturing defects were placed in the beam specimens. Incorporating defects into future training and testing sets would be recommended.

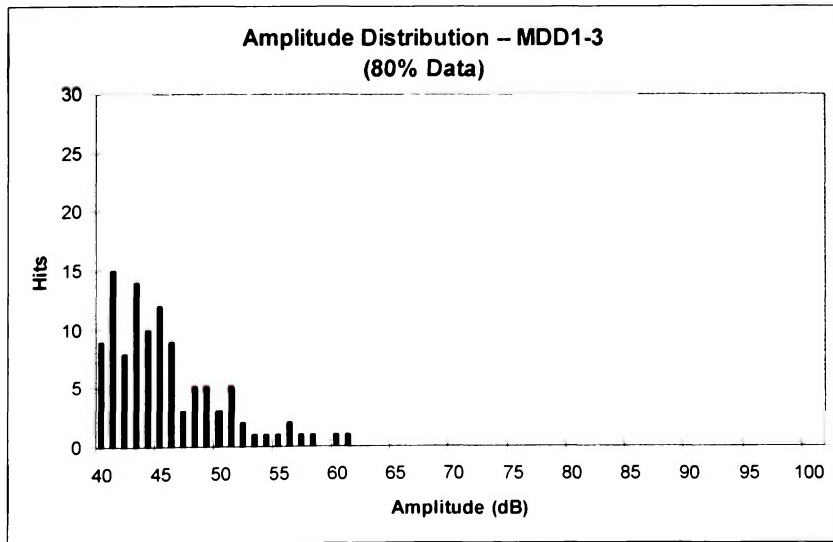
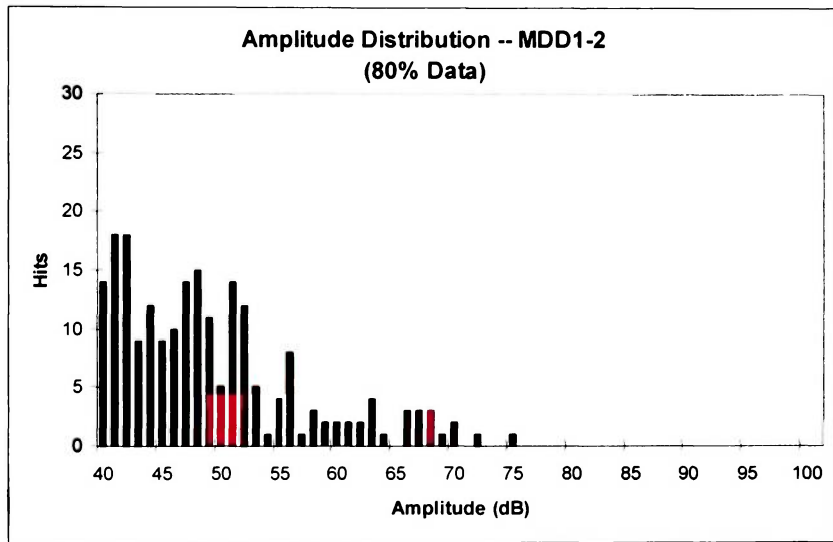
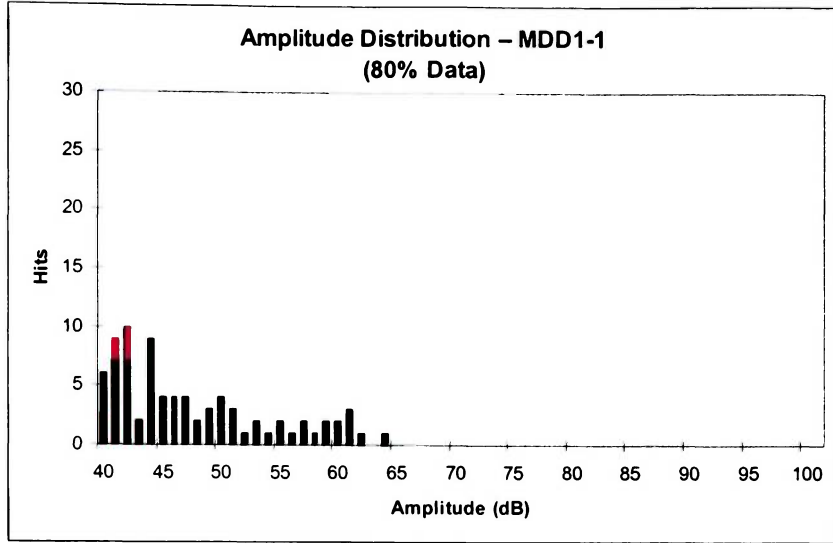
REFERENCES

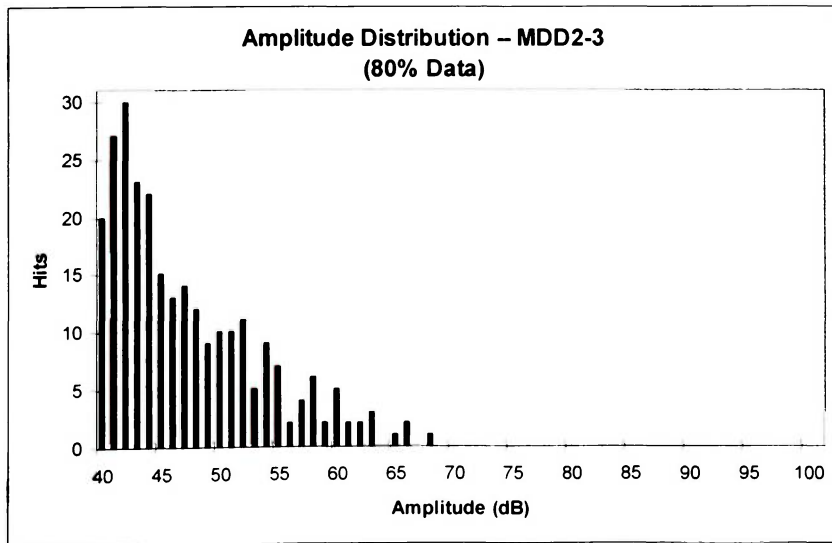
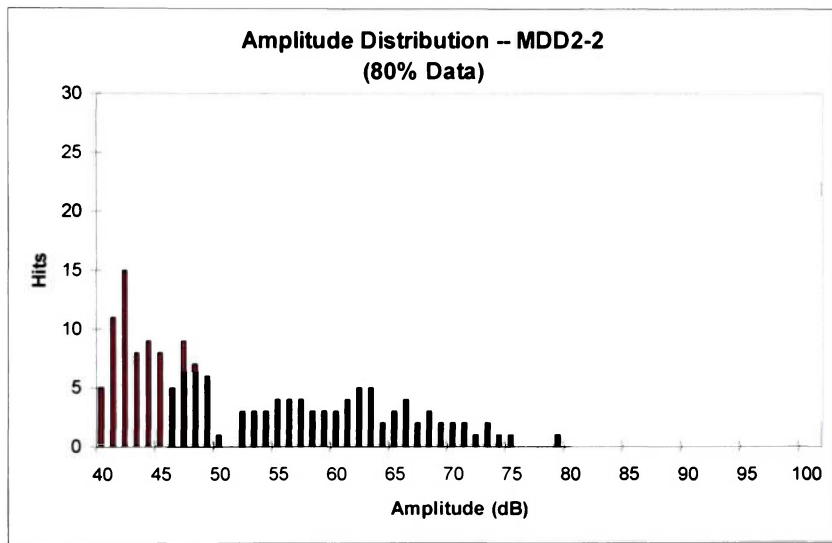
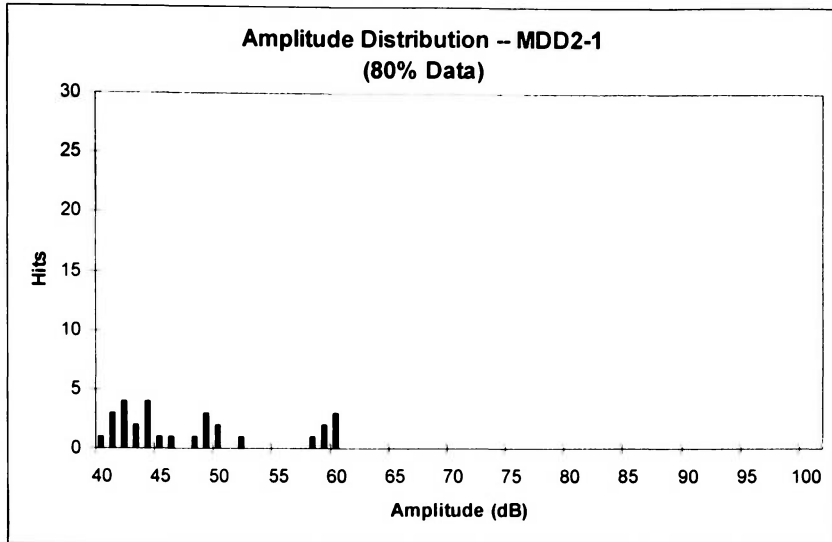
1. Hoskin, B., and Baker, A., *Composite Materials for Aircraft Structures*, American Institute of Aeronautics and Astronautics, Inc., 1986, pp. 1-7.
2. Scott, Ian G., *Basic Acoustic Emission*, Gordon and Breach Science, 1991, pp. 86-87.
3. Hill, Eric v. K., Walker, James L., and Rowell, Ginger H., "Burst Pressure Prediction in Graphite/Epoxy Pressure Vessels Using Neural Networks and Acoustic Emission Amplitude Data," *Materials Evaluation*, Volume 54, No. 6, 1996, pp. 748-754.
4. Fisher, Marcus E. and Hill, Eric v. K., "Burst Pressure Prediction of Filament Wound Composite Pressure Vessels Using Acoustic Emission," *Materials Evaluation*, Volume 56, No. 12, 1998, pp. 1395-1401.
5. Fatzinger, Edward C. and Hill, Eric v. K., "Neural Network Prediction of Ultimate Loads in Fiberglass/Epoxy I-Beams from Acoustic Emission Data," *Journal of Composites Technology & Research*.
6. Kouvarakos, M., and Hill, Eric v. K., "Isolating Tensile Failure Mechanisms in Fiberglass/Epoxy from Acoustic Emission Signal Parameters," *Materials Evaluation*, Volume 54, No. 9, 1996, pp. 1025-1031.
7. Pollock, Adrian A., "Acoustic Emission Inspection," *Metals Handbook*, Ninth Edition, Volume 17, 1989, pp. 278-294.
8. Hill, Eric v. K., "Predicting Burst Pressures in Filament Wound Composite Pressure Vessels Using Acoustic Emission Data," *Materials Evaluation*, Volume 50, No. 12, 1992, pp. 1439-1445.
9. Walker, James L., and Hill, Eric v. K., "An Introduction to Neural Networks: A Tutorial," First International Conference on Nonlinear Problems in Aviation and Aerospace, S. Sivasundaram, Editor, Embry-Riddle Aeronautical University Press, Daytona Beach, Florida, 1997, pp. 667-672.
10. Holman, J. P., *Experimental Methods for Engineers*, Second Edition, McGraw-Hill, 1971, p. 56.
11. Graham, Lloyd J., "Acoustic Emission Signal Analysis for Failure Mode Identification," 1980 Paper Summaries, ASNT National Spring Conference, American Society for Nondestructive Testing, Columbus, OH, 1980, pp. 74-79.

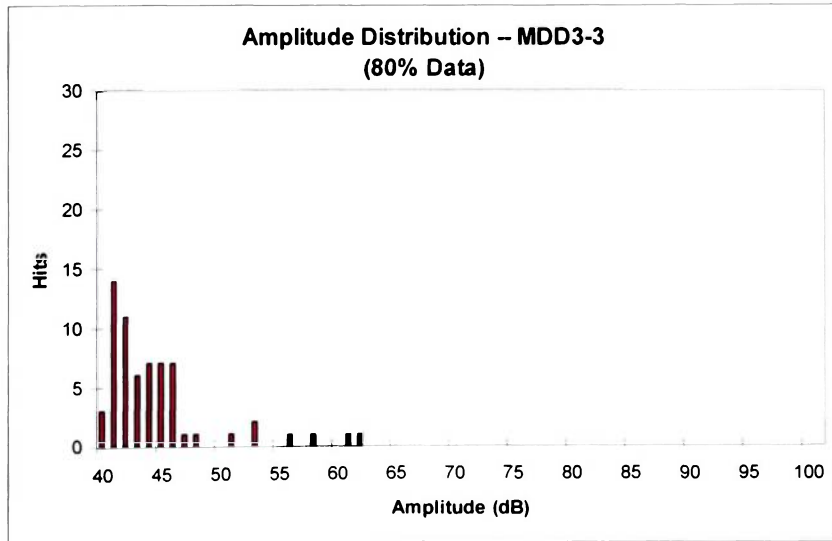
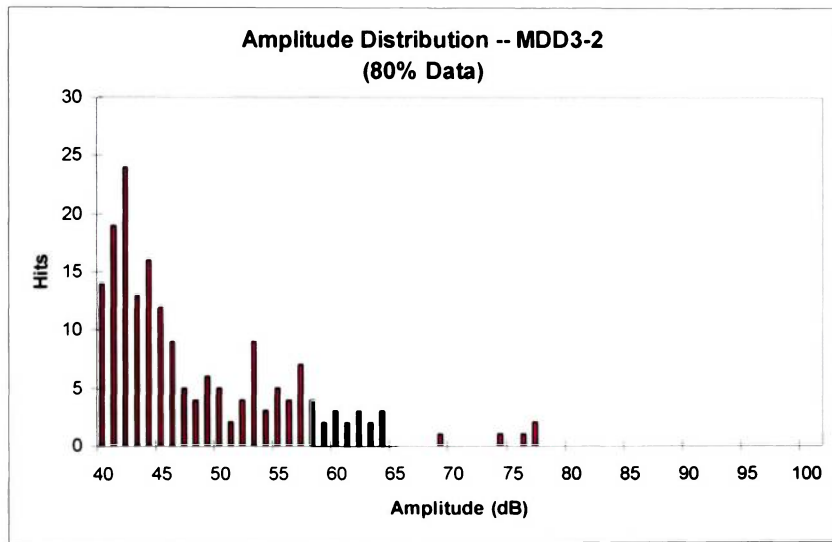
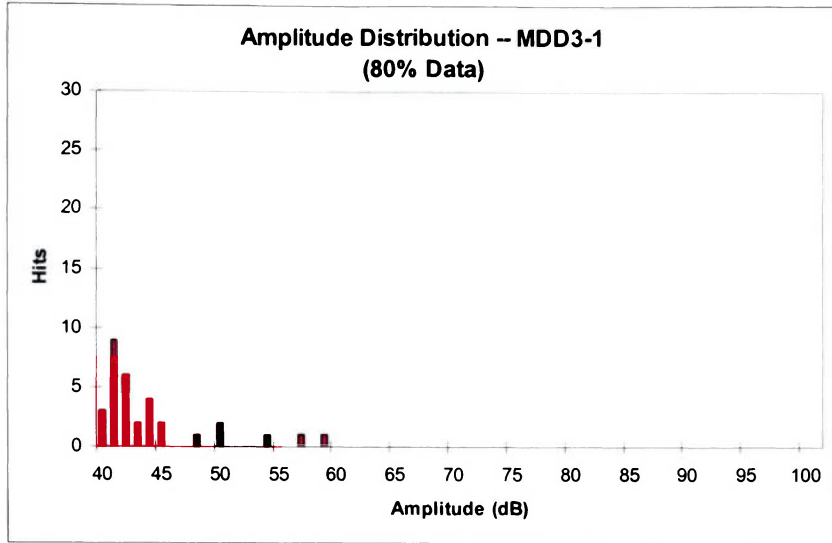
BIBLIOGRAPHY

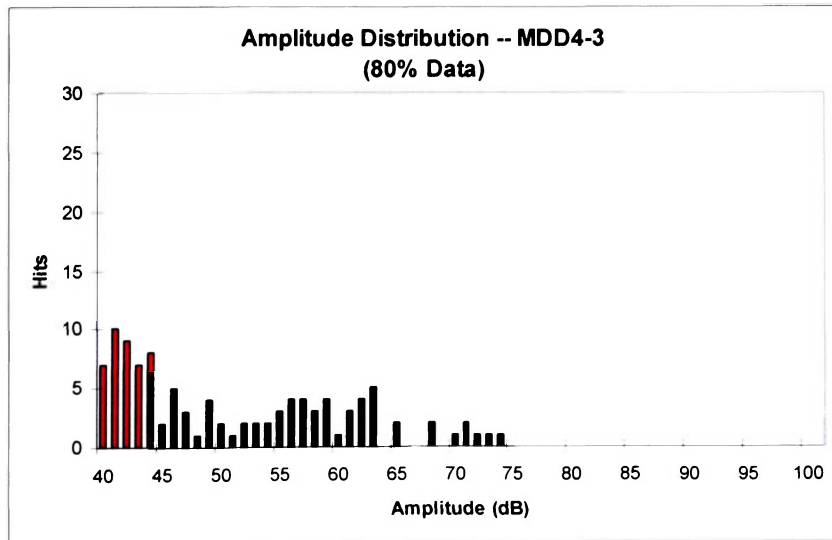
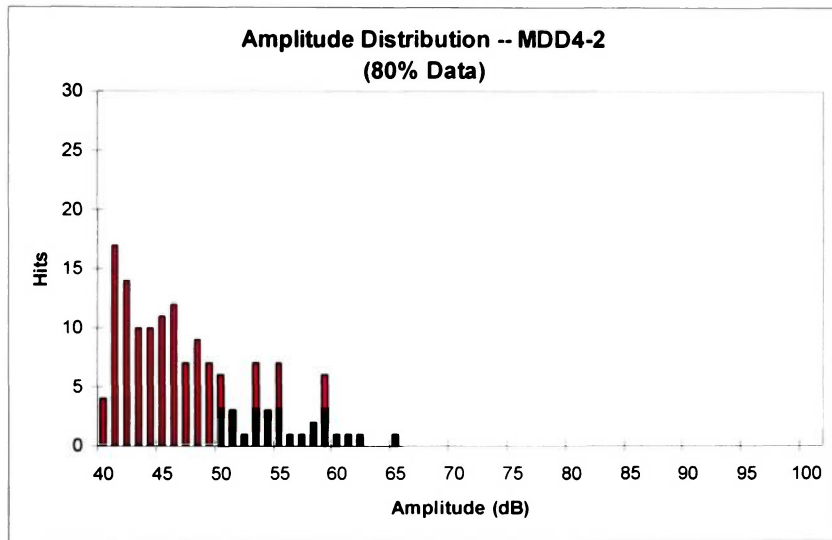
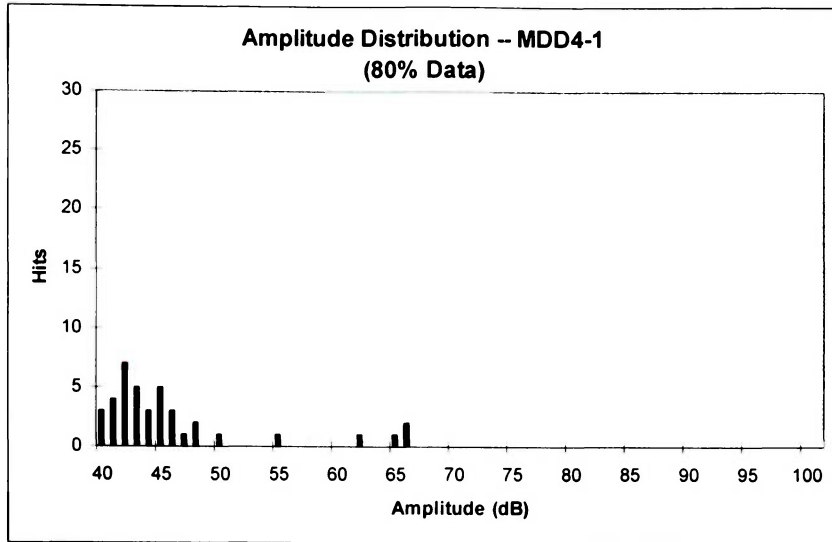
1. Barbero, Ever J., *Introduction to Composite Materials Design*, Taylor & Francis, Pennsylvania, 1999
2. Fausett, Laurene, *Fundamentals of Neural Networks, Architecture, Algorithms, and Applications*, Englewood Cliffs, New Jersey, 1994.
3. Miller, Ronnie K. and McIntire, Paul, Editors, *Nondestructive Testing Handbook, Volume 5 of Acoustic Emission Testing*, Second Edition. American Society for Nondestructive Testing (ASNT), 1987.
4. NeuralWare, Incorporated, Reference Guide NeuralWorks Professional II/Plus and NeuralWorks Explorer, 1995.
5. Physical Acoustics Corporation, DiSP User's Manual, Revision 1, Princeton NJ, 2001.
6. Strong, A. Brent, *Fundamentals of Composites Manufacturing: Materials, Methods, and Applications*, Society of Manufacturing Engineers, Michigan, 1989.
7. Swanson, Stephen R., *Introduction to Design and Analysis with Advanced Composite Materials*, Upper Saddle River, New Jersey, 1997.
8. Triola, Mario F., *Elementary Statistics*, Reading, Massachusetts, 1998.
9. Wasserman, Philip D., *Neural Computing Theory and Practice*, Van Nostrand Reinhold, New York, 1989.

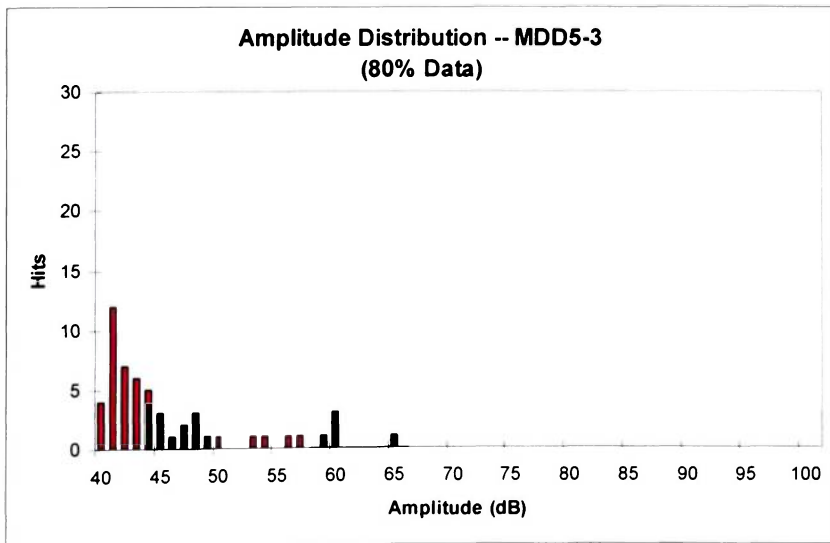
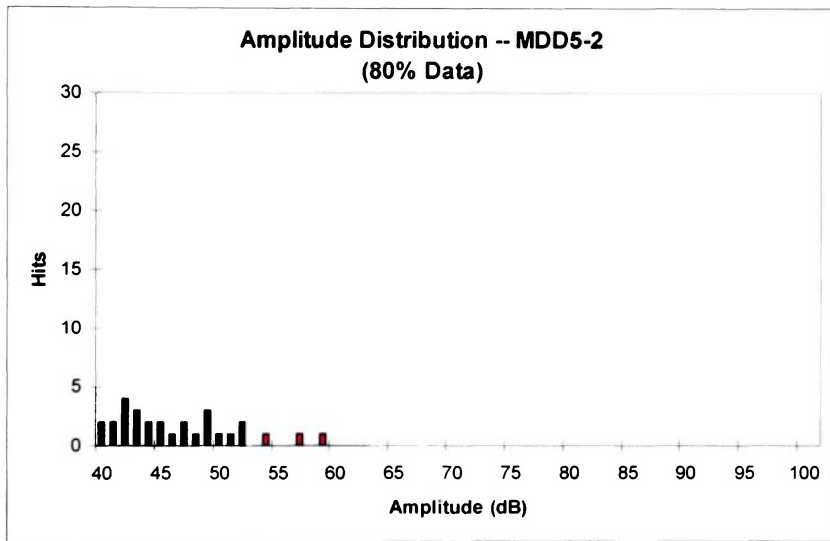
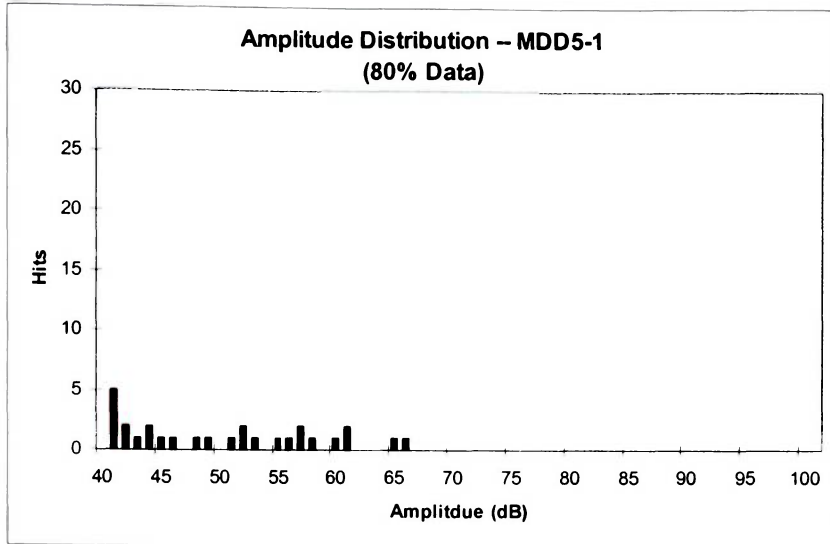
APPENDIX A
ACOUSTIC EMISSION DATA PLOTS

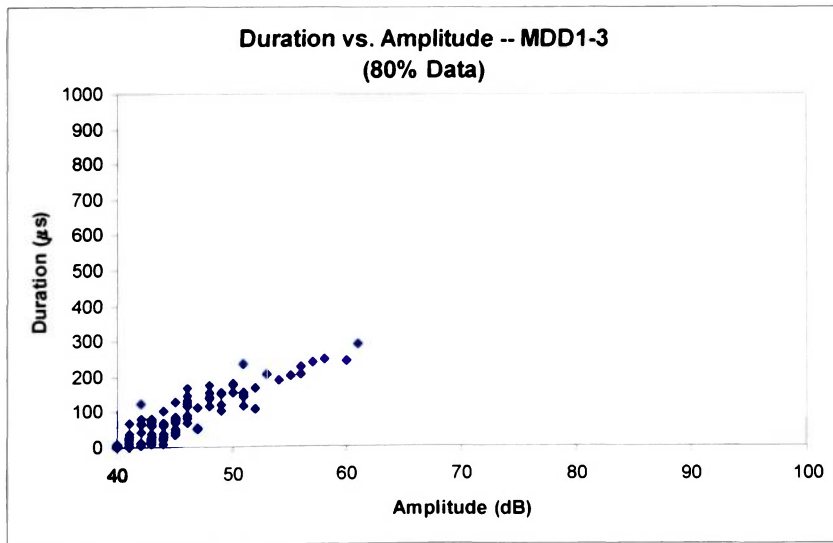
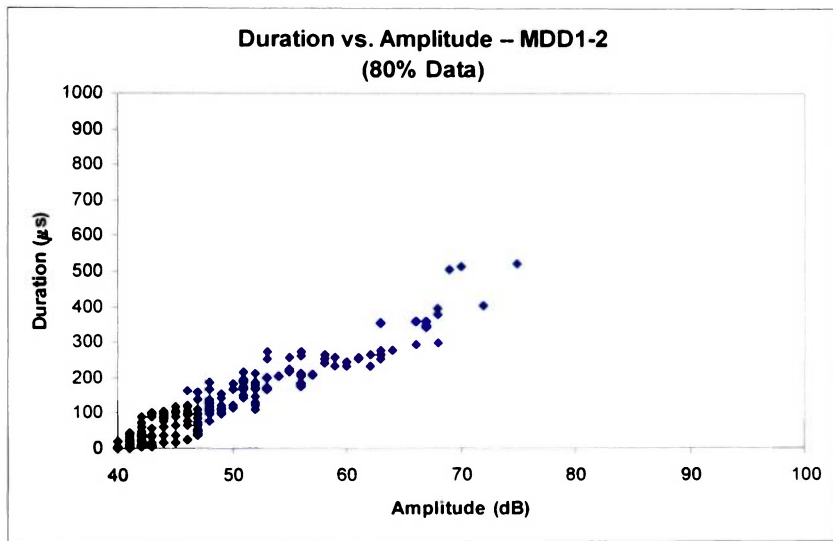
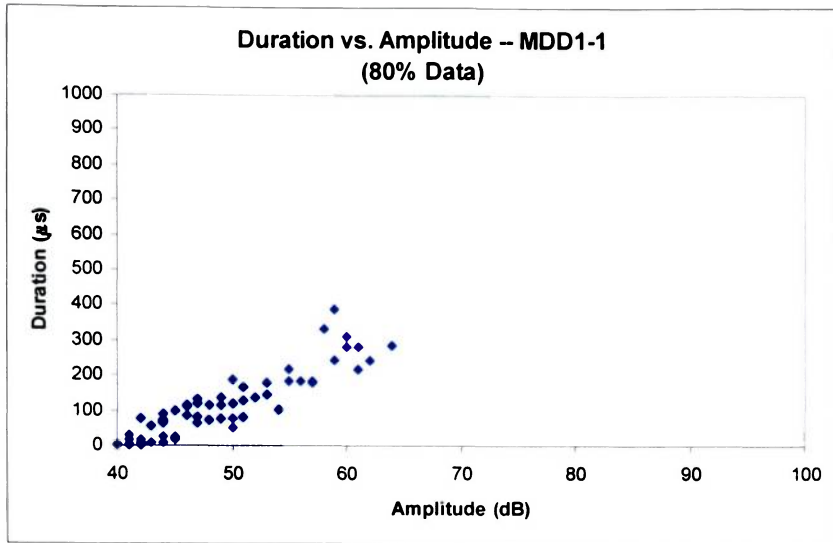


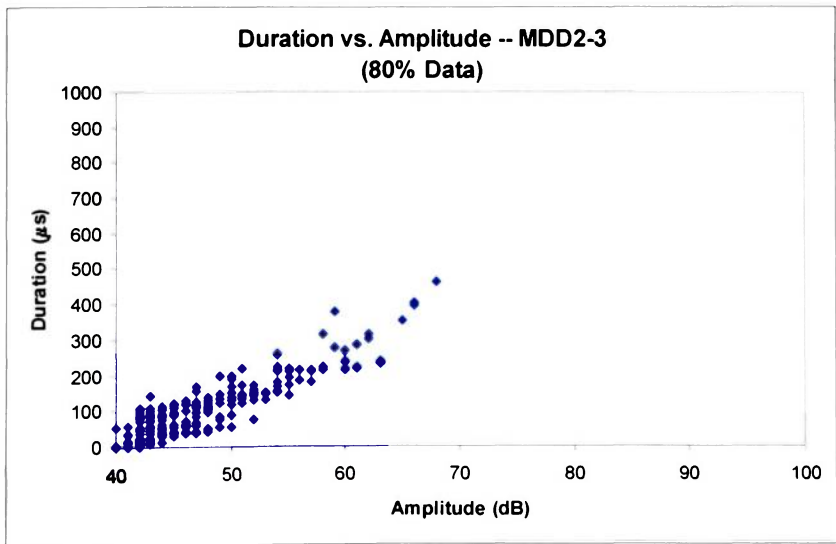
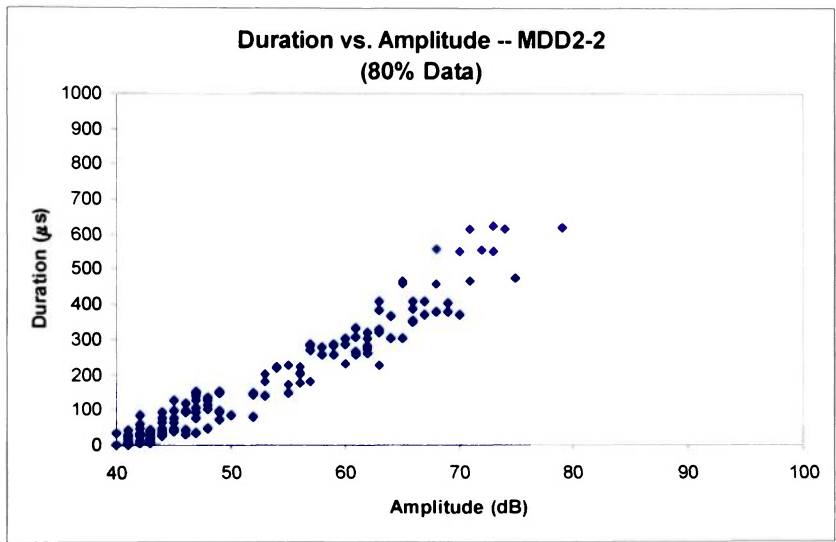
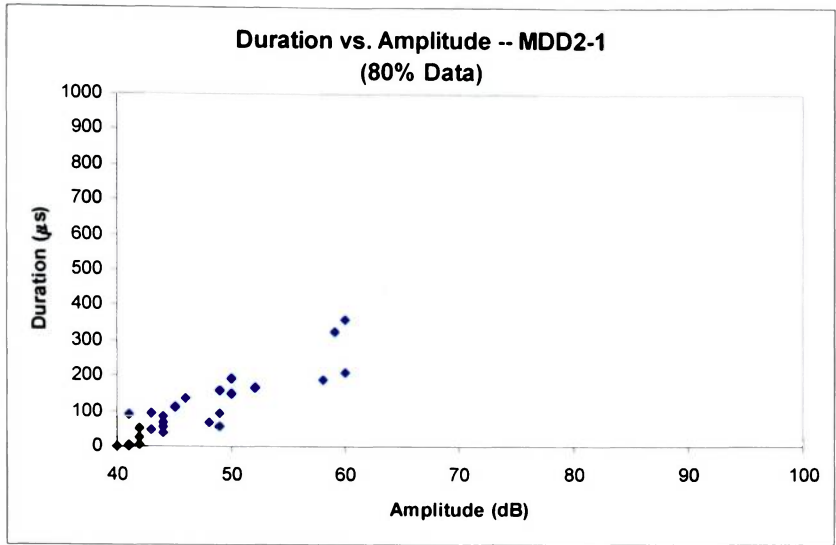


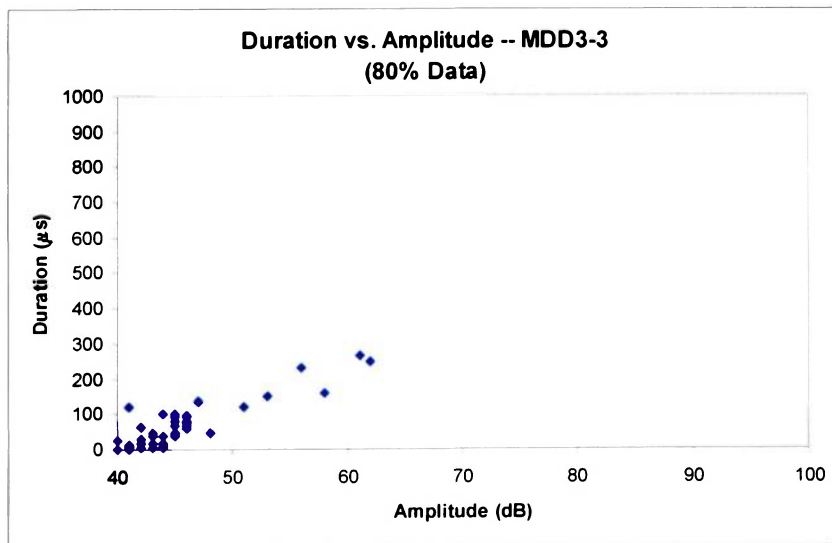
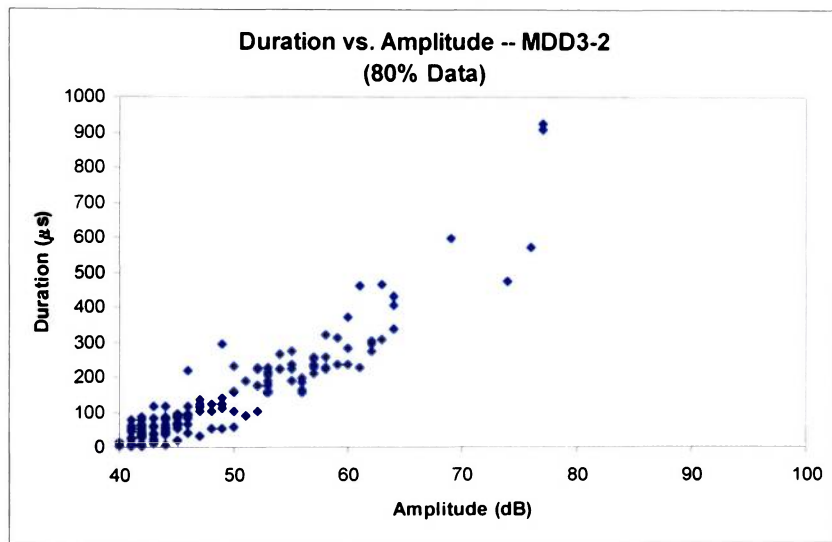
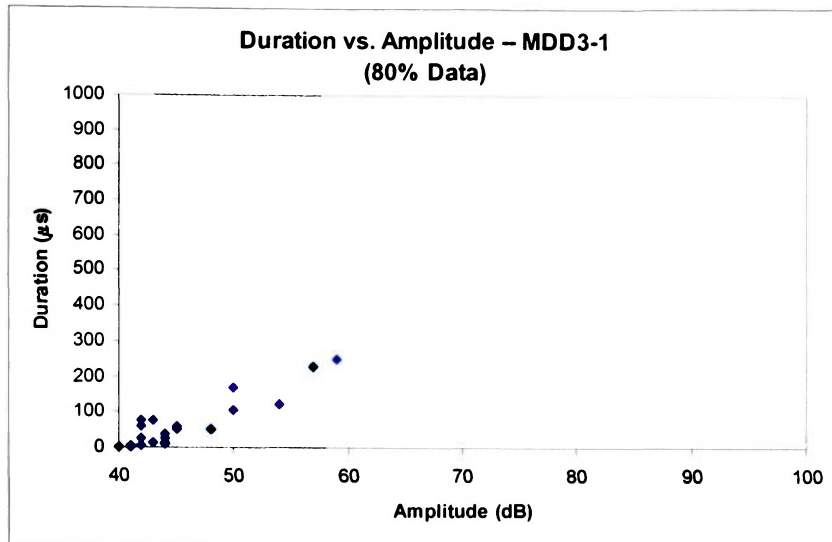


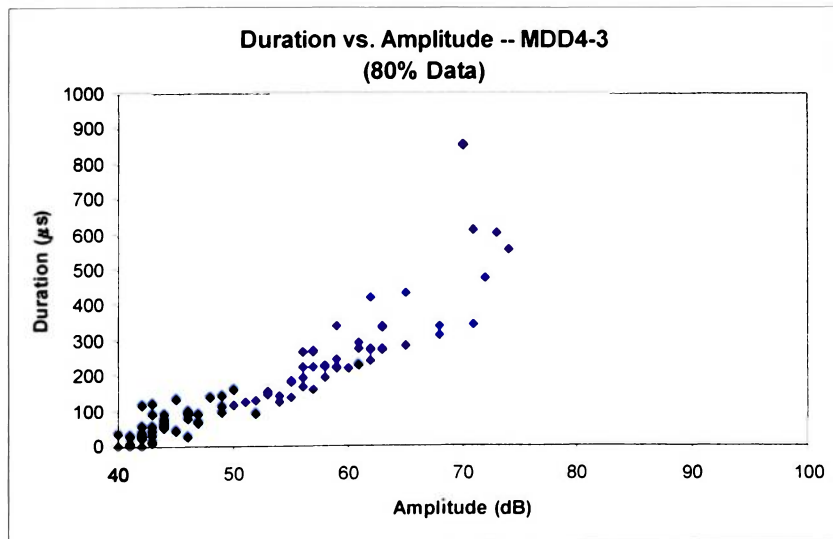
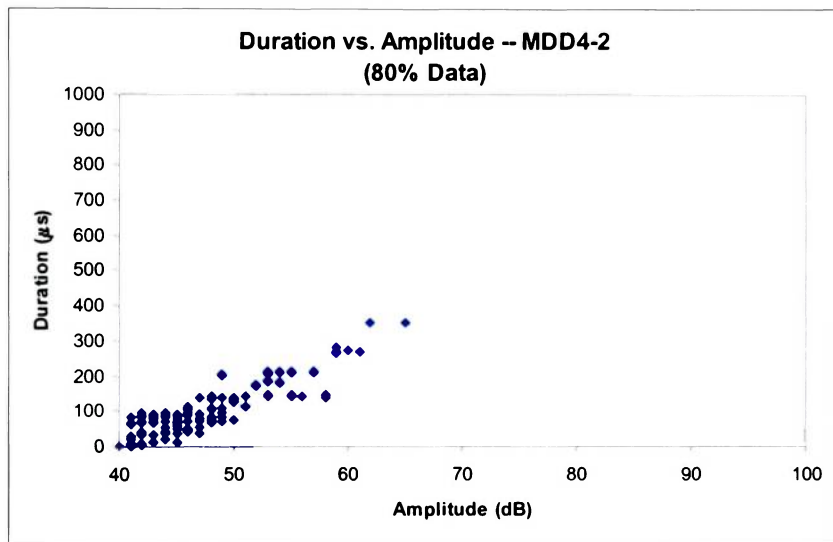
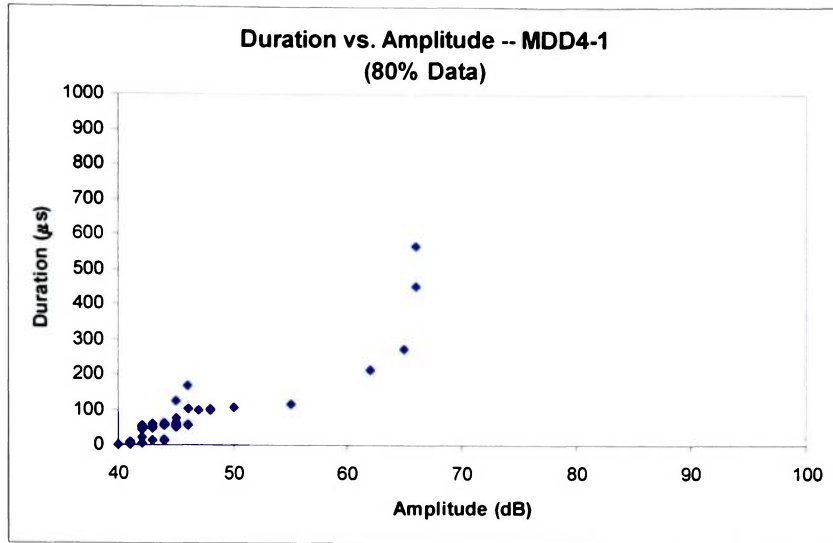


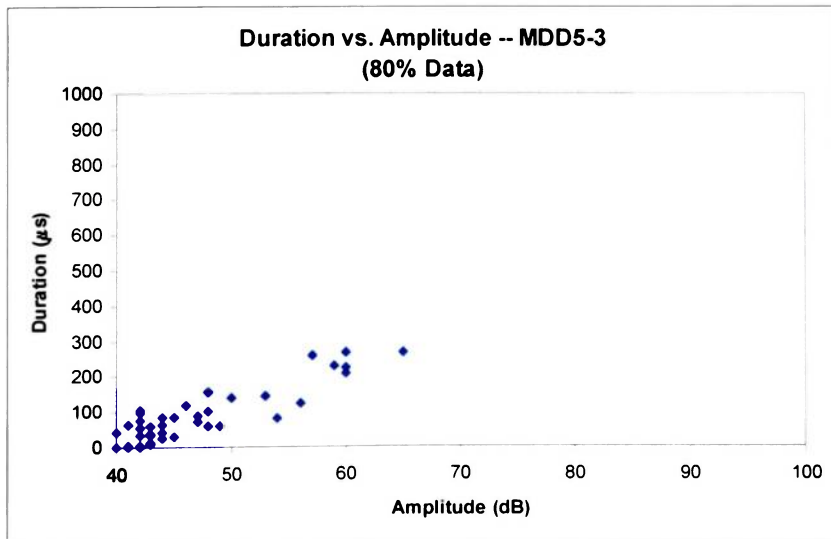
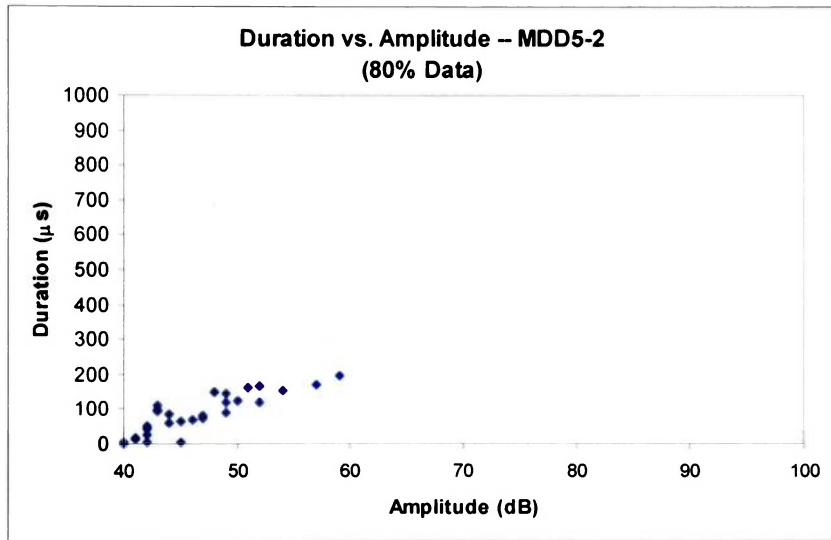
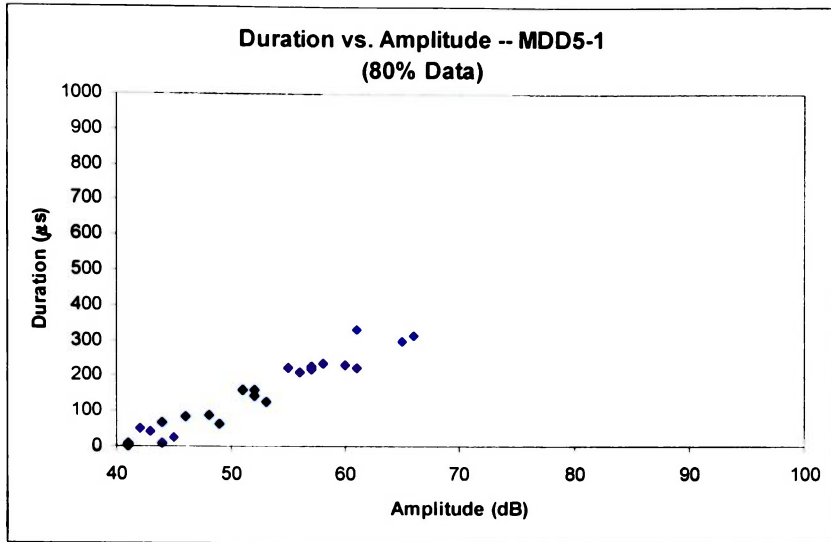


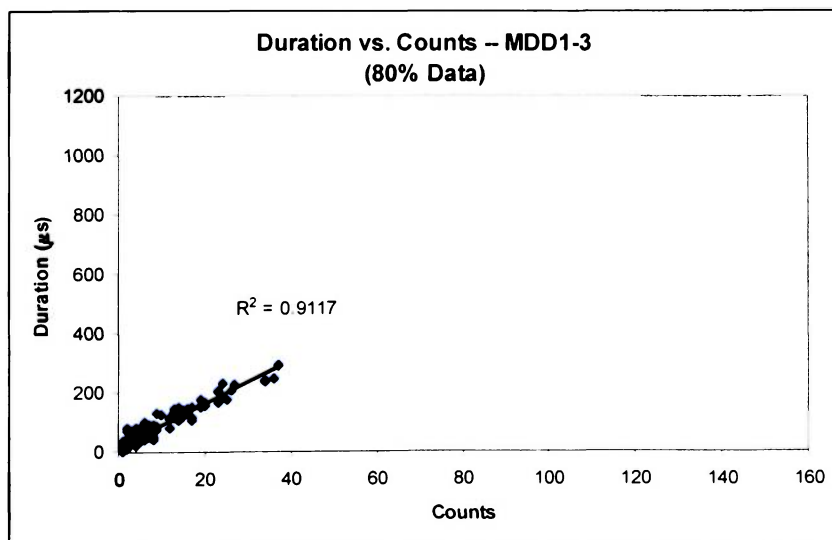
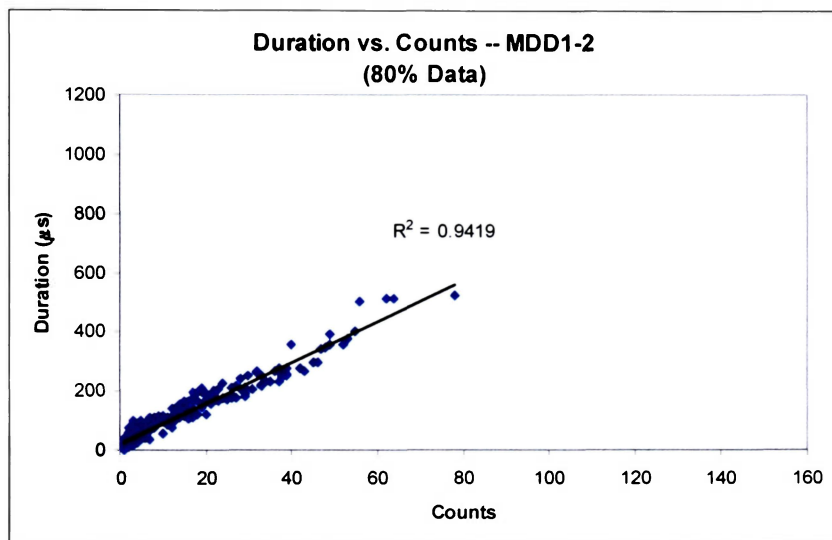
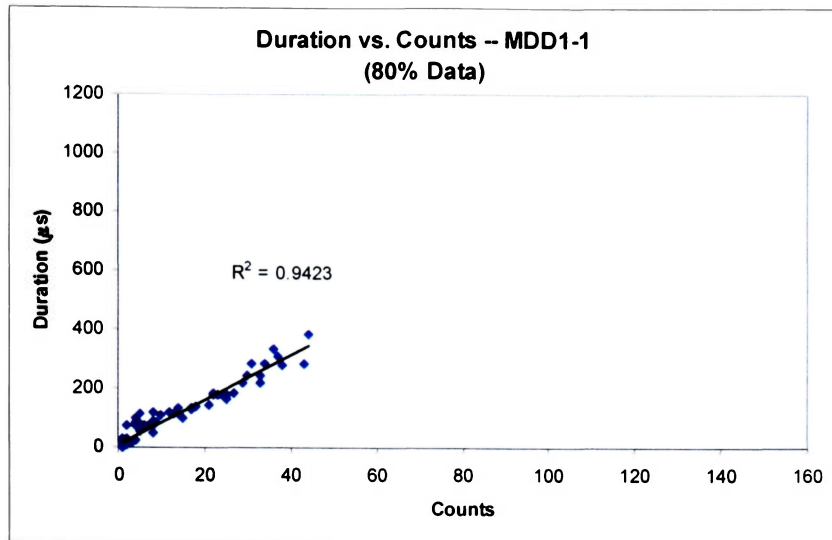


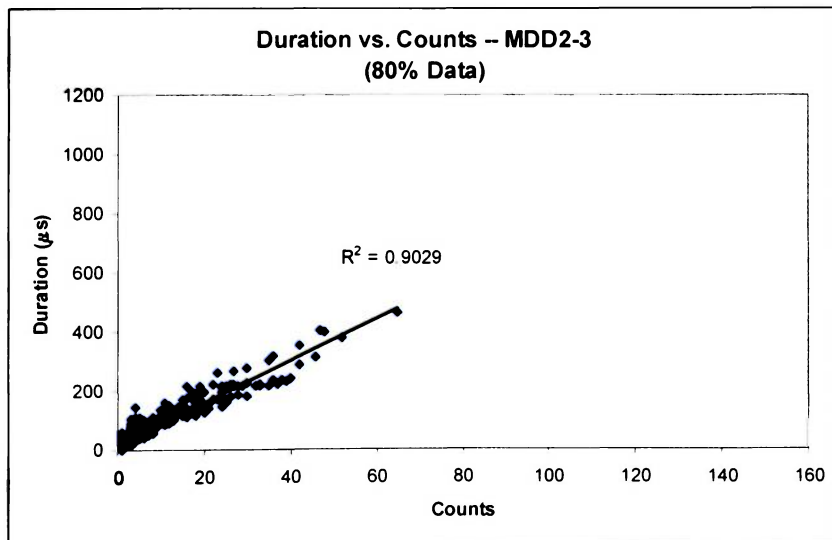
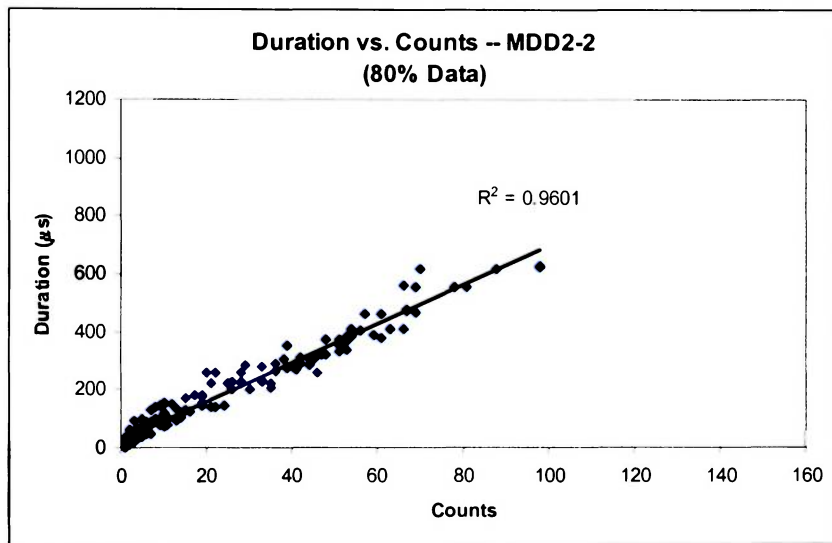
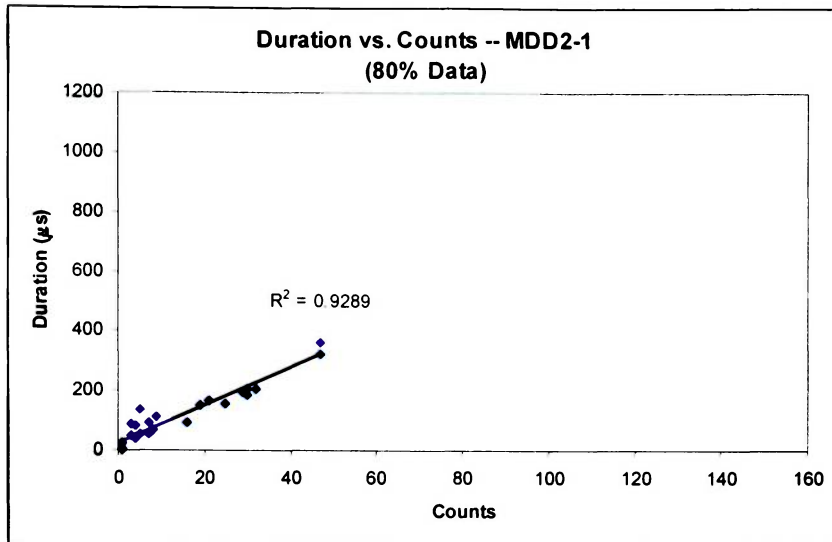


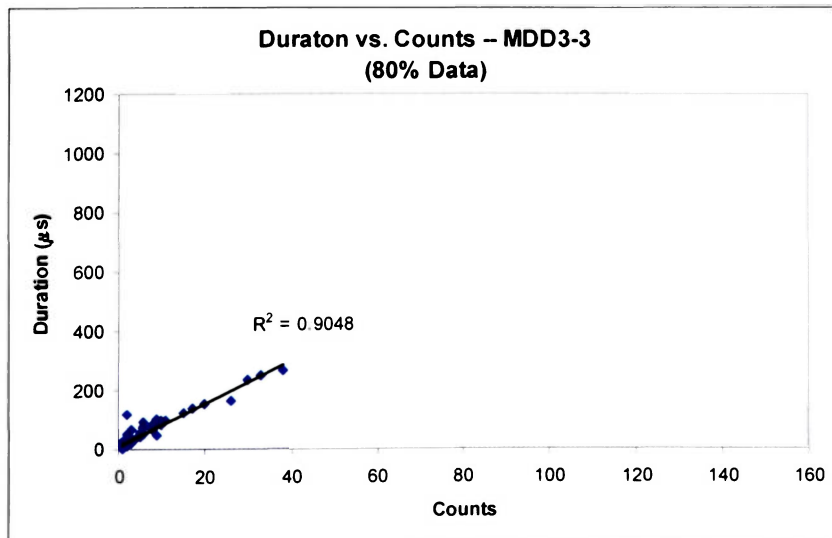
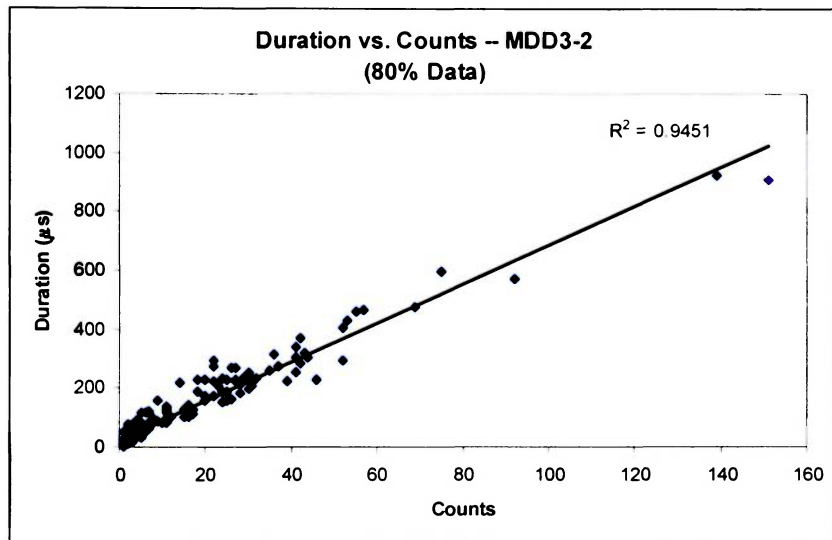
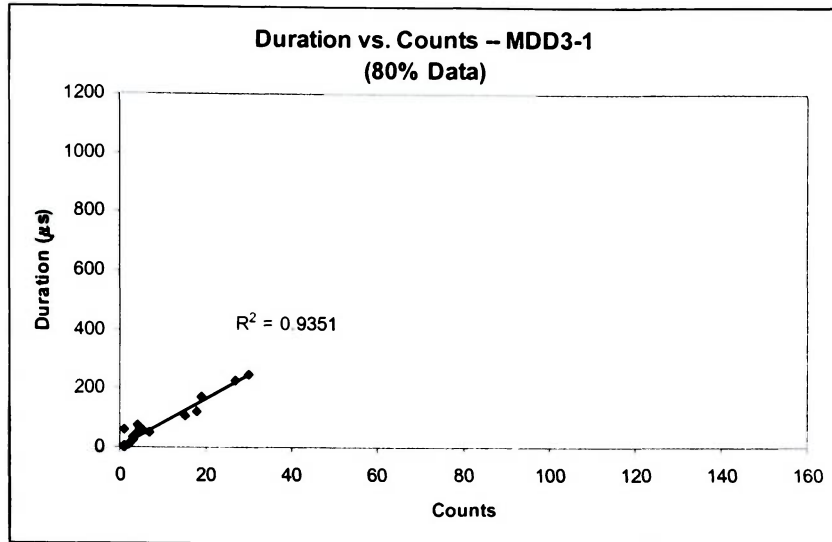


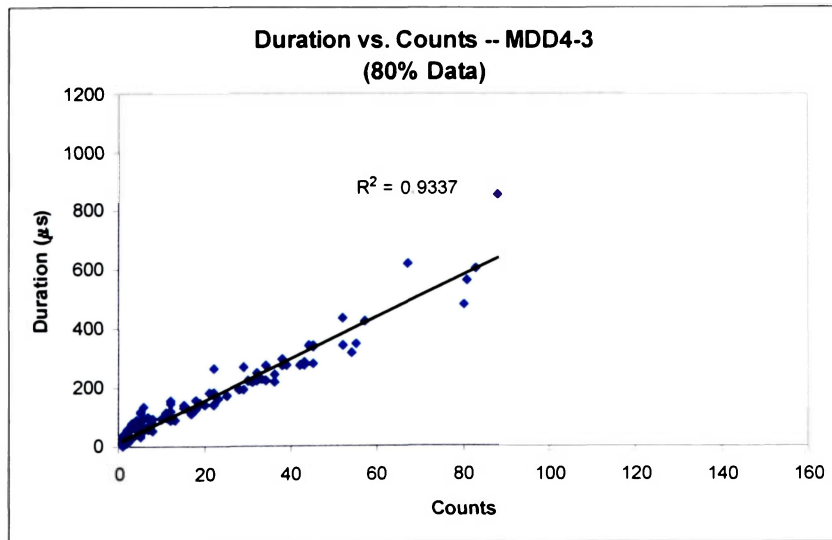
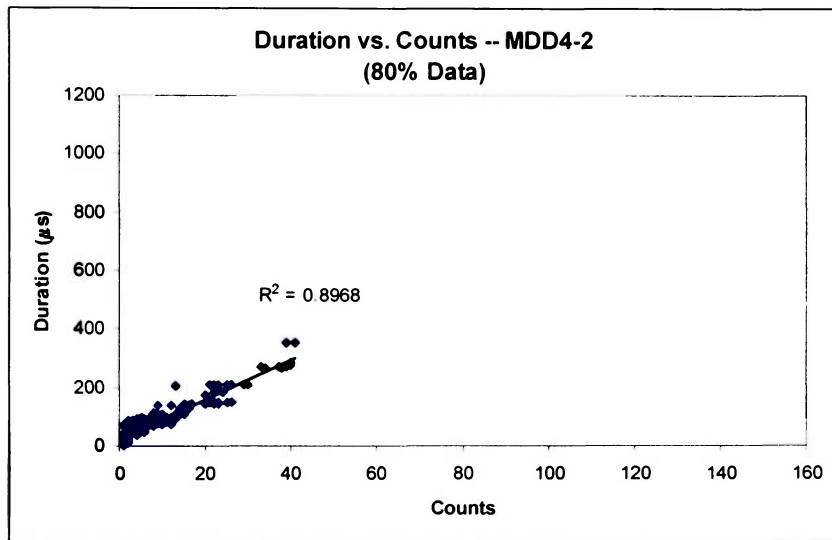
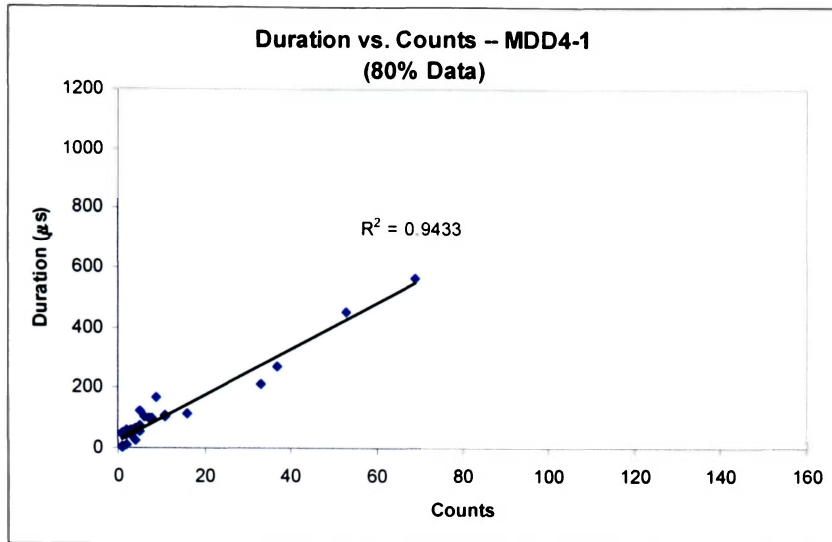


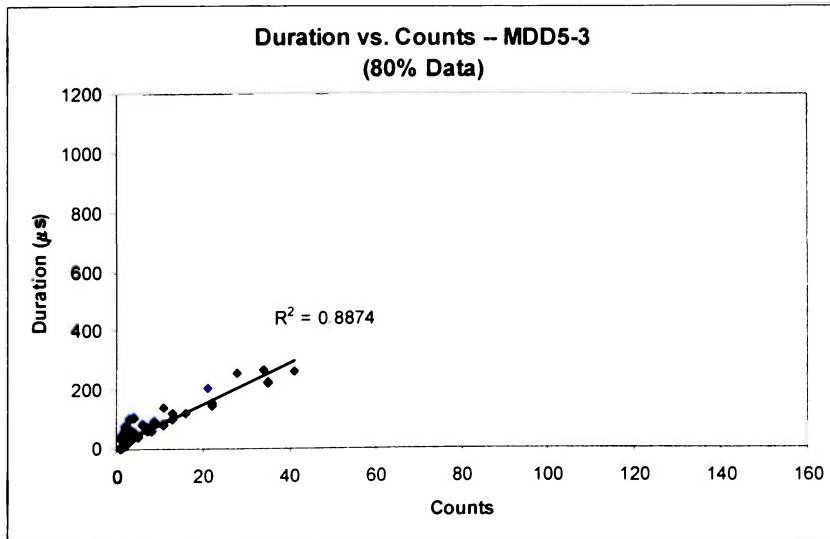
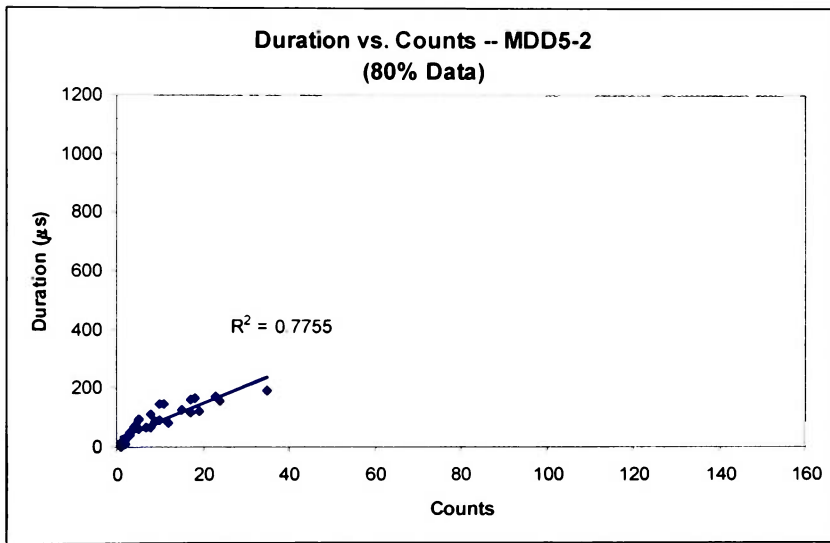
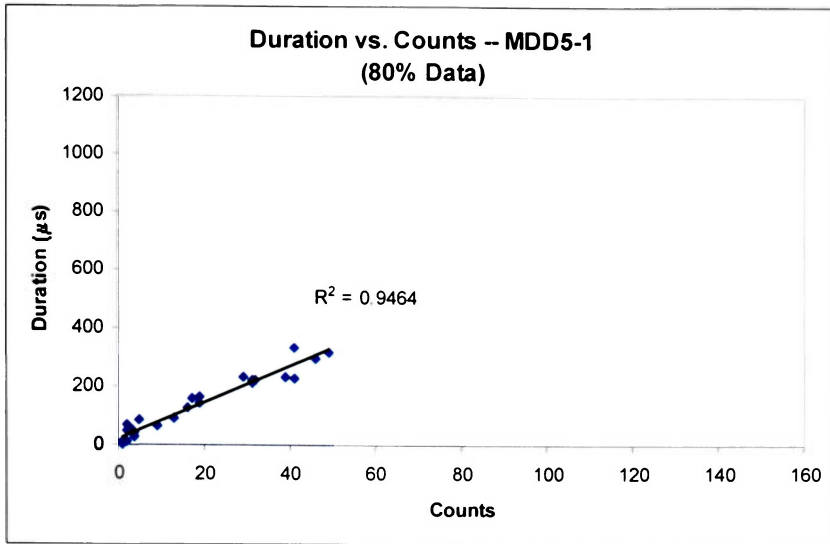












APPENDIX B
NEURAL NETWORK PARAMETER DEFINITIONS

Backpropagation Neural Networks

NeuralWare defines the dialog box components and their functions as:

PEs

These text fields specify the number of processing elements (nodes) for each layer in the back-propagation network. Input corresponds to the input or bottom layer, Hid 1 through Hid 3 correspond to three hidden layers (usually you will only need one or two hidden layers), and Output corresponds to the output or top layer. The number of PEs in the input and output layers depend on the number of data fields in each data vector in your training data. The number of outputs depends on what information you want your network to provide (and requires a matching number of data fields for desired output).

LCoef

The LCoef fields correspond to Learning Rate (in the learn and recall schedule, learn section) for each of the hidden layers and the output layer. Learning coefficients are used by the learning and recall schedule, and (if the Default Schedule box in the learning and recall schedule is not checked) the Back-propagation command constructs a separate learning and recall schedule for each hidden layer and the output layer. LCoef works in conjunction with the Trans. Pt. and LCoef ratio values to configure the learning and recall schedules. The value entered in a layer's LCoef field corresponds to the first Coefficient 1 value in the learning and recall schedule (shown in the following table). The Trans. Point corresponds to the learn count value set in column 1 in the schedule. The learn count for the subsequent columns are heuristically set to 3, 7, 15 and 31 times the learn count you enter in the Trans. Point field; i.e., the intervals between transition points increase exponentially. The LCoef Ratio sets the amount to divide the LCoef value by for the first transition. This defines an exponential decay which is sampled at subsequent transition points. For example, if you set a learning coefficient of 0.5 and an LCoef Ratio of 0.5, the values for the various columns in the schedule will be:

Column 1 0.5 (the LCoef value)

Column 2 0.25 (the previous column value divided by the LCoef ratio value of 2)

Column 3 0.0625 (the previous column value divided by 4)

Column 4 0.00391 (the previous column value divided by 16)

Column 5 0.00002 (the previous column value divided by 256)

Momentum

The Momentum field value is also used in configuring the learning and recall schedules for the hidden and output layers. Basically, momentum works by adding a tendency for weights to continue to change in the direction they are already changing. For back-propagation networks, momentum is represented in the learning and recall schedules by learning Momentum. The Momentum value interacts with the Trans. Pt. and LCoef Ratio exactly as do the LCoef field values described above.

Trans. Pt.

See the explanation in the LCoef section above.

LCoef Ratio

See the explanation in the LCoef section above.

F' Offset

This is a value added to the derivative of the transfer function prior to calculating the value to back propagate from each PE. For a Sigmoid or Tanh transfer function a value of about 0.1 helps networks from getting saturated. The symptom of a saturated network is large weights and summation values. It is difficult for a saturated network to learn any further.

Learn Rule

The Learn Rule scroll window allows you to select the learning rule that is applied to all layers in the back-propagation network. The learning rule specifies how connection weights are changed during the learning process. The six learning rules available are:

- Delta-rule, which is the standard back-propagation learning rule.
- Normalized-cumulative delta-rule - a rule which accumulates weight changes and updates the weights at end of epoch. It is normalized so that the learning rate is independent of the epoch size.
- Extended delta-bar-delta
- Quickprop
- Maxprop
- Delta-bar-delta

You can use the Layer/Edit tool to assign learning rules on a layer-by-layer basis. For most applications we recommend trying extended delta-bar-delta, normalized-cumulative delta-rule, or with fast learning, the delta-rule.

Transfer

The transfer function scroll window allows you to specify a transfer function that is used for all layers in the network. The transfer function is a non-linear function that transfers the internally generated sum for each PE to a potential output value. Available transfer functions are:

Linear
Hyperbolic tangent (TanH)
Sigmoid
DNNA
Sine

Learn

The Learn Browse button is used to select the training data file for the network. Alternatively, you can type the filename into the text entry field. Input data files have a file extension of .nna, .txt or any other extension, but they must have an extension (typing "myfile" becomes "myfile.nna").

Recall/Test

The Recall/Test Browse button allows you to select a data file for recall and test execution. Alternatively, you can type the filename into the text entry field. Like the Learn data file, Recall/Test input data files also have a file extension of .nna, .txt or any other extension.

Connect Prior

For each layer, makes connections from all previous layers.

Auto-Associative

If Auto-Associative is checked, NeuralWorks sets the number of output PEs to the number of input PEs and, when training, uses the input data as the desired output. Backpropagation networks can use this mode for applications such as data compression or noise filtering.

Linear Output

Linear Output overrides the selected transfer function and forces a linear transfer function for the output layer. The linear transfer function takes the current sum for each PE as its output.

SoftMax Output

Softmax forces both a linear transfer function and a “softmax output function”. You should use this only on applications that meet these two criteria:

- The application is a classification problem
- The components of the desired output add up to one.

Fast Learning

Selecting this check box uses a fast version of the back-propagation control strategy. We also recommend that you use the delta-rule learning rule for fast learning.

Gaussian Init

Attaches the Gaussian noise function (instead of the uniform noise function) to all layers in the network. This function is used for both initialization and noise. Three things must occur before a layer actually uses the noise function:

- The control strategy must call for a noise function.
- The learn and/or recall temperature value in the learning and recall schedule must be set to a non-zero value. By default, NeuralWorks sets these to zero.
- A noise function must be attached to the layer. Uniform noise adds a random number within a specified range to each PE summation value in the layer. The range for random numbers is plus or minus one percent of the temperature value. The random number for the noise value is different for each PE in the layer. Gaussian noise is similar to uniform noise, except that the distribution of random numbers within the range is along a bell curve, i.e., more concentrated toward the middle of the range than at the ends.

Minimal Config.

Minimal Config. provides the minimum number of weight fields required for a learning rule. For instance, a minimum configuration of the normalized cumulative delta rule will have two weight fields. Not checking this would provide the normalized cumulative delta-rule with three weight fields, the third being used for momentum. You should only check this box if your computer system does not have enough memory for the default configuration.

MinMax Table

Selecting this check box causes NeuralWorks to compute the low and high values for each data field in the selected data files and store these in a MinMax Table. When data is presented to the network, it is scaled to the network ranges using the MinMax table and the network range values (set through the IO/Parameters command).

Bipolar Inputs

Used in conjunction with a MinMax table. If this is selected and a MinMax Table is used, input values are mapped to lie between -1.0 and 1.0. If it is not selected and a MinMax Table is used, input values are mapped to between 0.0 and 1.0.

Cascade Learn

This activates “Cascade Learn” in the Run menu which implements a form of Cascade Correlation training. In such networks, PEs in the hidden layer are incrementally added, and are trained individually to take responsibility for any remaining output error. Each hidden unit receives input from both the input buffer and from all prior hidden PEs. If you use this option, you still need to specify a number of hidden PEs. This provides a pool of PEs which the Cascade Learning algorithm will activate one by one until no more improvement occurs. Any disabled PEs left after convergence occurs can be purged using the “Utilities/Purge” menu option.

Epoch

Epoch size is used for all learning rules except Delta-Rule. However, even if the Delta-Rule is being used, it is useful to set an epoch since certain instruments (such as RMS Error graph) update their calculations at the end of an epoch.

Set Epoch From File

This will set the epoch to the number of vectors in the training file. However, it is recommended that the Epoch size should be LESS THAN the number of vectors in the training file, and for most problems an upper bound of 200 for the epoch is valid.

RMS Error

Choosing this instrument creates a strip chart instrument that shows the RMS error of the output layer. For some applications (though not all) as learning progresses you should see this graph slowly converge to an error near zero. You can activate the convergence threshold in the RMS instrument, which, when reached, will stop network training. Use the Graph/Edit tool to activate Convergence Criterion and change the convergence threshold value. The convergence threshold is set to 0.001 by default.

Kohonen Self Organizing Maps

NeuralWare defines the dialog box components and their functions as:

Inputs

This sets the # of Inputs going into the SOM.

Rows and # Cols

Sets the # of neurons in the rows and columns of the two-dimensional grid. Use large (10x10 or greater) to find number of categories. If the number of failure mechanisms are known, use a number of Rows and Columns whose product is equal to greater than known number of mechanisms.

Hidden and Output

These are for if you want a mapping network at the output of the SOM. Set the values to 0 if no hidden layer is created.

SOM Steps

This sets the number of learning iterations for the SOM. (If you use the Set Epoch From File button, # SOM Steps is set to 30 times the number of hits in the training file.)

LCoef

Sets the first item under LCoef to be the desired learning rate for the Kohonen layer.

Beta

Beta is used in the equation to update the estimate of how frequently a Kohonen neuron wins. If you use the Set Epoch From File button the default value for Beta is set based on the number of training cases: $\text{Beta} = 1 / (\# \text{ training hits})$

Gamma

Gamma is used in conjunction the frequency estimation to determine a bias term which is added to the Euclidean distance function for the *i*th Kohonen neuron. The effect of this is to favor neurons which have not won recently, and this encourages all the Kohonen neurons to be utilized.

Coord. Layer

This creates a layer above the two-dimensional Kohonen layer which outputs the feature map as a pair of coordinates. These coordinates are normalized to lie between -1.0 and 1.0.

Output Network

This creates a back-propagation layer above the two-dimensional coordinate layer or above the coordinate layer. Use this option if you have desired outputs to which you want to map.

MinMax Table

If selected, NeuralWorks will compute the low and high values for each data field in the selected data files, and store these in a MinMax Table.

Interpolate

If this is checked, the top three winners in the two-dimensional Kohonen layer are calculated at each Kohonen learn step.

Neighborhood

1. Choose between a Diamond shaped or Square shaped neighborhood, or Alternating square and diamond shaped neighborhoods.
2. Choose the neighborhood sizes by setting the Starting Width and Ending Width. We recommend that you start with a large width (7 or above) and progress to a small width (1 or 3) by the end.
3. Optionally select horizontal or vertical wrap-around.

Learn

Select a training file using the Learn Browse button. Alternatively, you can type the filename into the text entry field.

Recall/Test

Select a test file using the Recall/Test Browse button. Alternatively, you can type the filename into the text entry field.

Connect Prior

If selected, and your network has a hidden layer, the output layer is fully connected from the Kohonen or coordinate layer as well as from the hidden layer.

Connect Bias

If selected, this creates connections from the bias neuron to the mapping layers.

Linear Output

If selected, this overrides the selected transfer function and forces a linear transfer function for the output layer.

SoftMax Output

If selected, this option forces a linear transfer function and a SoftMax output function. This should only be used with classification type problems in which the desired output is categorical in nature, and the components of each desired output vector sum to 1.

Epoch

The epoch size is used for all learning rules in the mapping layers except the delta-rule. However, even if the delta-rule is being used, it is useful to set an epoch since certain instruments (such as RMS Error graph) update their calculations at the end of an epoch. Set Epoch From File button will set the epoch to the number of hits in the training file.

Learn Rule

- Delta-rule, which is the standard back-propagation learning rule.
- Norm-cum-delta, a rule which accumulates weight changes and updates the weights at end of epoch. It is normalized so that the learning rate is independent of the epoch size.
- Ext DBD (extended delta-bar-delta)
- QuickProp
- MaxProp
- Delta-bar-delta

The chosen rule is used for each layer of the network.

Transfer

- Linear
- TanH (hyperbolic tangent)
- Sigmoid
- DNNA

The tool recommends that you use either the TanH or sigmoid transfer functions. The chosen function is used for each layer of the network.

APPENDIX C

BACKPROPAGATION NEURAL NETWORK RESULTS

50	61	13	1	0.2	0.15	0.4	7000	0.5	0.05	0.03	0.03	
49	61	13	1	0.15	0.15	0.4	7000	0.5	0.05	0.03	0.03	
48	61	13	1	0.1	0.15	0.4	7000	0.5	0.05	0.03	0.03	
47	61	13	1	0.3	0.15	0.7	7000	0.5	0.05	0.03	0.03	
46	61	13	1	0.3	0.15	0.65	7000	0.5	0.05	0.03	0.03	
45	61	13	1	0.3	0.15	0.6	7000	0.5	0.05	0.03	0.03	
44	61	13	1	0.3	0.15	0.55	7000	0.5	0.05	0.03	0.03	
43	61	13	1	0.3	0.15	0.5	7000	0.5	0.05	0.03	0.03	
42	61	13	1	0.3	0.15	0.45	7000	0.5	0.05	0.03	0.03	
41	61	13	1	0.3	0.15	0.4	7000	0.5	0.05	0.03	0.03	
Network Number	Inputs	Hidden 1	Output	L. Coef.	Momentum	Trans. Pt.	L. Coef. Ratio	F. Offset	Learn Rule	Transfer	Epoch	RMS Error

40	61	13	1	0.3	0.15	0.36	7000	0.5	0.05	0.03	0.03	
39	61	13	1	0.3	0.15	0.3	7000	0.5	0.05	0.03	0.03	
38	61	13	1	0.3	0.15	0.25	7000	0.5	0.05	0.03	0.03	
37	61	13	1	0.3	0.15	0.2	7000	0.5	0.05	0.03	0.03	
36	61	13	1	0.3	0.15	0.4	15000	0.5	0.05	0.03	0.03	
35	61	13	1	0.3	0.15	0.4	14000	0.5	0.05	0.03	0.03	
34	61	13	1	0.3	0.15	0.4	13000	0.5	0.05	0.03	0.03	
33	61	13	1	0.3	0.15	0.4	12000	0.5	0.05	0.03	0.03	
32	61	13	1	0.3	0.15	0.4	11000	0.5	0.05	0.03	0.03	
31	61	13	1	0.3	0.15	0.4	10000	0.5	0.05	0.03	0.03	
Network Number	Inputs	Hidden 1	Output	L. Coef.	Momentum	Trans. Pt.	L. Coef. Ratio	F. Offset	Learn Rule	Transfer	Epoch	RMS Error

30	61	13	1	0.3	0.15	0.4	9000	0.5	0.05	0.03	0.03	
29	61	13	1	0.3	0.15	0.4	8000	0.5	0.05	0.03	0.03	
28	61	13	1	0.3	0.15	0.4	7000	0.5	0.05	0.03	0.03	
27	61	13	1	0.3	0.15	0.4	6000	0.5	0.05	0.03	0.03	
26	61	13	1	0.3	0.15	0.4	5000	0.5	0.05	0.03	0.03	
25	61	13	1	0.3	0.15	0.4	7500	0.5	0.05	0.03	0.03	
24	61	13	1	0.3	0.15	0.4	7500	0.5	0.05	0.03	0.03	
23	11	13	1	0.3	0.15	0.4	7500	0.5	0.15	0.03	0.03	
22	23	23	1	0.3	0.15	0.4	10000	0.5	0.1	0.03	0.03	
21	61	22	1	0.3	0.15	0.4	10000	0.5	0.1	0.03	0.03	
Network Number	Inputs	Hidden 1	Output	L. Coef.	Momentum	Trans. Pt.	L. Coef. Ratio	F. Offset	Learn Rule	Transfer	Epoch	RMS Error

20	61	21	1	0.3	0.15	0.4	10000	0.5	0.1	0.03	0.03	
19	61	20	1	0.3	0.15	0.4	10000	0.5	0.1	0.03	0.03	
18	61	19	1	0.3	0.15	0.4	10000	0.5	0.1	0.03	0.03	
17	61	18	1	0.3	0.15	0.4	10000	0.5	0.1	0.03	0.03	
16	61	17	1	0.3	0.15	0.4	10000	0.5	0.1	0.03	0.03	
15	61	16	1	0.3	0.15	0.4	10000	0.5	0.1	0.03	0.03	
14	61	15	1	0.3	0.15	0.4	10000	0.5	0.1	0.03	0.03	
13	61	14	1	0.3	0.15	0.4	10000	0.5	0.1	0.03	0.03	
12	61	13	1	0.3	0.15	0.4	10000	0.5	0.1	0.03	0.03	
11	61	12	1	0.3	0.15	0.4	10000	0.5	0.1	0.03	0.03	
Network Number	Inputs	Hidden 1	Output	L. Coef.	Momentum	Trans. Pt.	L. Coef. Ratio	F. Offset	Learn Rule	Transfer	Epoch	RMS Error

10	61	11	1	0.3	0.15	0.4	10000	0.5	0.1	0.03	0.03	
9	61	10	1	0.3	0.15	0.4	10000	0.5	0.1	0.03	0.03	
8	61	9	1	0.3	0.15	0.4	10000	0.5	0.1	0.03	0.03	
7	61	8	1	0.3	0.15	0.4	10000	0.5	0.1	0.03	0.03	
6	61	7	1	0.3	0.15	0.4	10000	0.5	0.1	0.03	0.03	
5	61	6	1	0.3	0.15	0.4	10000	0.5	0.1	0.03	0.03	
4	61	5	1	0.3	0.15	0.4	10000	0.5	0.1	0.03	0.03	
3	61	4	1	0.3	0.15	0.4	10000	0.5	0.1	0.03	0.03	
2	61	3	1	0.3	0.15	0.4	10000	0.5	0.1	0.03	0.03	
1	61	2	1	0.3	0.15	0.4	10000	0.5	0.1	0.03	0.03	
Network Number	Inputs	Hidden 1	Output	L. Coef.	Momentum	Trans. Pt.	L. Coef. Ratio	F. Offset	Learn Rule	Transfer	Epoch	RMS Error

Network Number	51	52	53	54	55	56	57	58	59	60
Inputs	61	61	61	61	61	61	61	61	61	61
Hidden 1	13	13	13	13	13	13	13	13	13	13
Output	1	1	1	1	1	1	1	1	1	1
L. Coef.	0.25	0.3	0.35	0.4	0.45	0.5	0.3	0.3	0.3	0.3
	0.15	0.15	0.15	0.15	0.15	0.15	0.05	0.1	0.15	0.2
Momentum	0.4	0.4	0.4	0.4	0.4	0.4	0.4	0.4	0.4	0.4
Trans. Pt.	7000	7000	7000	7000	7000	7000	7000	7000	7000	7000
L. Coef. Ratio	0.5	0.5	0.5	0.5	0.5	0.5	0.5	0.5	0.5	0.5
F' Offset	0.05	0.05	0.05	0.05	0.05	0.05	0.05	0.05	0.05	0.05
Learn Rule	NCD	NCD	NCD	NCD	NCD	NCD	NCD	NCD	NCD	NCD
Transfer	tanH	tanH	tanH	tanH	tanH	tanH	tanH	tanH	tanH	tanH
Epoch	21	21	21	21	21	21	21	21	21	21
RMS Error	0.03	0.03	0.03	0.03	0.03	0.03	0.03	0.03	0.03	0.03

Network Number	61	62	63	64	65	66	67	68	69	70
Inputs	61	61	61	61	61	61	61	61	61	61
Hidden 1	13	13	13	13	13	13	13	13	13	13
Output	1	1	1	1	1	1	1	1	1	1
L. Coef.	0.3	0.3	0.3	0.3	0.3	0.3	0.3	0.3	0.3	0.3
	0.25	0.3	0.15	0.15	0.15	0.15	0.15	0.15	0.15	0.15
Momentum	0.4	0.4	0.4	0.4	0.4	0.4	0.4	0.4	0.4	0.4
Trans. Pt.	7000	7000	7000	7000	7000	7000	7000	7000	7000	7000
L. Coef. Ratio	0.5	0.5	0.1	0.15	0.2	0.25	0.3	0.35	0.4	0.45
F' Offset	0.05	0.05	0.05	0.05	0.05	0.05	0.05	0.05	0.05	0.05
Learn Rule	NCD	NCD	NCD	NCD	NCD	NCD	NCD	NCD	NCD	NCD
Transfer	tanH	tanH	tanH	tanH	tanH	tanH	tanH	tanH	tanH	tanH
Epoch	21	21	21	21	21	21	21	21	21	21
RMS Error	0.03	0.03	0.03	0.03	0.03	0.03	0.03	0.03	0.03	0.03

Network Number	71	72	73	74	75	76	77	78	79	80
Inputs	61	61	61	61	61	61	61	61	61	61
Hidden 1	13	13	13	13	13	13	13	13	13	13
Output	1	1	1	1	1	1	1	1	1	1
L. Coef.	0.3	0.3	0.3	0.3	0.3	0.3	0.3	0.3	0.3	0.3
	0.15	0.15	0.15	0.15	0.15	0.15	0.15	0.15	0.15	0.15
Momentum	0.4	0.4	0.4	0.4	0.4	0.4	0.4	0.4	0.4	0.4
Trans. Pt.	7000	7000	7000	7000	7000	7000	7000	7000	7000	7000
L. Coef. Ratio	0.5	0.55	0.6	0.65	0.7	0.75	0.8	0.85	0.9	0.35
F' Offset	0.05	0.05	0.05	0.05	0.05	0.05	0.05	0.05	0.05	0.05
Learn Rule	NCD	NCD	NCD	NCD	NCD	NCD	NCD	NCD	NCD	NCD
Transfer	tanH	tanH	tanH	tanH	tanH	tanH	tanH	tanH	tanH	tanH
Epoch	21	21	21	21	21	21	21	21	21	21
RMS Error	0.03	0.03	0.03	0.03	0.03	0.03	0.03	0.03	0.03	0.01

Network Number	81	82	83	84
Inputs	61	61	61	61
Hidden 1	13	13	13	13
Output	1	1	1	1
L. Coef.	0.3	0.3	0.3	0.3
	0.15	0.15	0.15	0.15
Momentum	0.4	0.4	0.4	0.4
Trans. Pt.	7000	7000	7000	7000
L. Coef. Ratio	0.35	0.35	0.35	0.35
F' Offset	0.05	0.05	0.05	0.05
Learn Rule	NCD	NCD	NCD	NCD
Transfer	tanH	tanH	tanH	tanH
Epoch	21	21	21	21
RMS Error	0.02	0.03	0.04	0.05

	Actual	Net 81	% Error	Net 82	% Error	Net 83	% Error	Net 84	% Error
Training Data	336	334.37	-0.484	333.58	-0.720	332.61	-1.008	331.67	-1.288
	372.5	372.45	-0.014	372.45	-0.013	372.41	-0.023	372.41	-0.024
	357.5	357.59	0.025	357.60	0.028	357.63	0.036	357.60	0.029
	312.5	312.14	-0.116	311.99	-0.163	311.89	-0.196	311.81	-0.221
	392.5	392.65	0.039	392.75	0.063	392.82	0.082	392.92	0.107
	375	377.04	0.543	378.11	0.829	378.98	1.060	379.90	1.307
	365	364.84	-0.044	364.91	-0.024	364.92	-0.023	365.10	0.027
Test Data	375	359.77	-4.061	359.45	-4.147	358.98	-4.273	358.54	-4.391
	312.5	326.72	4.550	326.05	4.335	325.36	4.116	324.67	3.893
	365	354.09	-2.990	354.16	-2.970	354.36	-2.916	354.70	-2.822
	327.5	334.50	2.137	334.49	2.136	334.37	2.099	334.30	2.076
	340	326.43	-3.992	325.50	-4.264	324.49	-4.561	323.51	-4.849
	363	361.98	-0.281	361.87	-0.313	361.56	-0.398	361.31	-0.465
	372.5	377.91	1.451	378.79	1.687	379.54	1.889	380.39	2.119
	367.5	382.76	4.152	383.11	4.248	383.34	4.311	383.64	4.393
	Worst	4.550	Worst	4.335	Worst	-4.561	Worst	-4.849	